

## ON STABLE, COMPLETE, AND SINGULARITY-FREE BOUNDARY INTEGRAL FORMULATIONS OF EXTERIOR STOKES FLOW\*

O. GONZALEZ†

**Abstract.** A new boundary integral formulation of the second kind for exterior Stokes flow is introduced. The formulation is stable, complete, singularity-free, and natural for bodies of complicated shape and topology. We prove an existence and uniqueness result for the formulation for arbitrary flows and illustrate its performance via several numerical examples using a Nyström method with Gauss–Legendre quadrature rules of different order.

**Key words.** Stokes equations, boundary integral equations, single-layer potentials, double-layer potentials, parallel surfaces, Nyström discretization

**AMS subject classifications.** 31B10, 35Q30, 76D07, 65R20

**DOI.** 10.1137/070698154

**1. Introduction.** In this article we study boundary integral formulations of exterior Stokes flow problems around arbitrary bodies with prescribed velocity data. For such problems it is well known that a formulation based on either of the classic single- or double-layer Stokes potentials is inadequate [29, 30]. A formulation based on the single-layer potential leads to a boundary integral operator which is unstable in the sense that its condition number is unbounded and incomplete in the sense that its range is deficient. Consequently, such a formulation is not optimal for numerical discretization and not capable of representing an arbitrary exterior flow. A formulation based on the double-layer potential leads to a boundary integral operator which is stable in the sense that its condition number is bounded but which is incomplete—even more so than the single-layer potential. Thus, in contrast to the single-layer case, a double-layer formulation is optimal for numerical discretization, but like the single-layer case, it is not capable of representing an arbitrary exterior flow.

Various authors have shown that a double-layer formulation can be modified so as to obtain completeness while retaining stability [14, 18, 20, 26, 28]. In Power and Miranda [28] it was shown that a complete formulation can be obtained by adding two classic singular flow solutions (a stokeslet and rotlet) to the double-layer potential, where the poles of the singular solutions are coincident and placed at an arbitrary location within the body. In Hebeker [14] it was shown that a complete formulation can be obtained by simply taking a positive linear combination of the classic single- and double-layer potentials. The approach of Power and Miranda has the desirable feature of being singularity-free in the sense that it leads to an integral equation involving only bounded integrands. In contrast, the approach of Hebeker leads to an integral equation with unbounded integrands. On the other hand, the approach of Power and Miranda is not natural for flows around bodies of complex shape or topology for which there is no distinguished point for the stokeslet and rotlet pole. In contrast, the approach of Hebeker is natural for flows around bodies of arbitrary shape.

---

\*Received by the editors July 23, 2007; accepted for publication (in revised form) August 21, 2008; published electronically January 14, 2009.

<http://www.siam.org/journals/siap/69-4/69815.html>

†Department of Mathematics, The University of Texas at Austin, 1 University Station C1200, Austin, TX 78712 (og@math.utexas.edu).

Here we introduce a new boundary integral formulation for exterior Stokes flow which combines the strengths of the Power and Miranda and the Hebeker formulations. The new formulation is stable, complete, singularity-free, and natural for bodies of complicated shape and topology. The formulation is made complete by virtue of a positive linear combination of single- and double-layer potentials and is made singularity-free by mapping the single-layer potential onto an appropriate parallel surface. We prove an existence and uniqueness result for the formulation for arbitrary flows and illustrate its performance via several numerical examples using a standard Nyström method based on Gauss–Legendre quadrature rules. Our results show that a standard method applied to the singularity-free formulation provides a simple and viable alternative to specialized methods required by classic formulations.

Classic boundary integral formulations of the Stokes equations involve weakly singular kernels that require special treatment. Such formulations can be treated with variants of the Nyström method which employ kernel-adapted product integration rules [3, 19] or coordinate transformations and projections which effectively remove the singularity [33]. Several types of Galerkin and collocation methods [3, 5, 6, 19] can also be applied to these formulations, as well as spectral Galerkin [2, 10, 12] and wavelet-based methods [1, 21, 32]. However, these approaches generally require basis functions that may be difficult to construct or which may exist only for certain classes of geometries. Moreover, they require special techniques for computing weakly singular integrals, which can be expensive. Here we show that such issues associated with classic formulations can be avoided in a simple and efficient way by a straightforward discretization of the singularity-free formulation.

The presentation is structured as follows. In section 2 we outline the Stokes equations for the steady flow of an incompressible viscous fluid in an exterior domain. In sections 3 and 4 we establish notation and collect several results on singular solutions and surface potentials for the Stokes equations that will be employed throughout our developments. In sections 5 and 6 we summarize, for purposes of comparison, the Hebeker and the Power and Miranda formulations of the exterior Stokes problem and highlight several of their properties. In section 7 we introduce our new formulation and establish its solvability properties for arbitrary data. In section 8 we describe a numerical discretization of our formulation using a standard Nyström method with an arbitrary quadrature rule. In section 9 we illustrate our approach with numerical examples and summarize our conclusions.

**2. The exterior Stokes problem.** In this section we define the boundary-value problem that we will study. We briefly outline standard assumptions which guarantee existence and uniqueness of solutions, and we introduce various flow quantities of interest that will be used to understand the properties of different boundary integral formulations.

**2.1. Problem formulation.** We consider the steady motion of a body of arbitrary shape through an incompressible viscous fluid at a low Reynolds number. In a body-fixed frame, we denote the body domain by  $B$ , the fluid domain exterior to the body by  $B_e$ , and the body-fluid interface by  $\Gamma$ . Given a body velocity field  $v : \Gamma \rightarrow \mathbb{R}^3$ , the basic problem is to find a fluid velocity field  $u : B_e \rightarrow \mathbb{R}^3$  and pressure field  $p : B_e \rightarrow \mathbb{R}$  which satisfy the classic Stokes equations, which in nondimensional form are

(2.1)



$$\begin{aligned}
 u_{i,jj} - p_{,i} &= 0, & x \in B_e, \\
 u_{i,i} &= 0, & x \in B_e, \\
 u_i &= v_i, & x \in \Gamma, \\
 u_i, p &\rightarrow 0, & |x| \rightarrow \infty.
 \end{aligned}$$

Equation (2.1)<sub>1</sub> is the local balance law of linear momentum for the fluid and (2.1)<sub>2</sub> is the local incompressibility constraint. Equation (2.1)<sub>3</sub> is the no-slip boundary condition which states that the fluid and body velocities coincide at each point of the boundary. The limits in (2.1)<sub>4</sub> are boundary conditions which are consistent with the fluid being at rest at infinity. Unless mentioned otherwise, all vector quantities are referred to a single basis and indices take values from one to three. Here and throughout we will use the usual conventions that a pair of repeated indices implies summation and that indices appearing after a comma denote partial derivatives.

**2.2. Solvability.** We assume  $B \cup \Gamma \cup B_e$  fills all of three-dimensional space,  $B$  is open and bounded, and  $B_e$  is open and connected. Moreover, we assume  $\Gamma$  consists of a finite number of disjoint, closed, bounded, and orientable components, each of which is a Lyapunov surface [13]. These conditions on  $\Gamma$  imply that standard results from potential theory for the Stokes equations may be applied [20, 26, 29]. Moreover, together with the continuity of  $v$ , they are sufficient to guarantee that (2.1) has a unique solution  $(u, p)$  with the following decay properties [9, 20]:

$$(2.2) \quad u_i = O(|x|^{-1}), \quad u_{i,j} = O(|x|^{-2}), \quad p = O(|x|^{-2}) \quad \text{as } |x| \rightarrow \infty.$$

The solution  $(u, p)$  is smooth in  $B_e$  but may possess only a finite number of bounded derivatives in  $B_e \cup \Gamma$  depending on the precise smoothness of  $\Gamma$  and  $v$ .

**2.3. Basic flow quantities.** The volume flow rate associated with a flow  $(u, p)$  and a given oriented surface  $S$  is defined by

$$(2.3) \quad Q = \int_S u_i(x) n_i(x) dA_x,$$

where  $n : S \rightarrow \mathbb{R}^3$  is a given unit normal field and  $dA_x$  denotes an infinitesimal area element at  $x \in S$ . When  $S$  is closed and bounded, we always choose  $n$  to be the outward unit normal. In this case,  $Q$  quantifies the volume expansion rate of the domain enclosed by  $S$ .

The fluid stress field associated with a flow  $(u, p)$  is a function  $\sigma : B_e \rightarrow \mathbb{R}^{3 \times 3}$  defined by

$$(2.4) \quad \sigma_{ij} = -p\delta_{ij} + u_{i,j} + u_{j,i},$$

where  $\delta_{ij}$  is the standard Kronecker delta symbol. For each  $x \in B_e$  the stress tensor  $\sigma$  is symmetric in the sense that  $\sigma_{ij} = \sigma_{ji}$ . The traction field  $f : S \rightarrow \mathbb{R}^3$  exerted by the fluid on a given oriented surface  $S$  is defined by

$$(2.5) \quad f_i = \sigma_{ij} n_j.$$

The resultant force  $F$  and torque  $T$ , about an arbitrary point  $c$ , associated with  $f$  are

$$(2.6) \quad F_i = \int_S f_i(x) dA_x, \quad T_i = \int_S \varepsilon_{ijk}(x_j - c_j) f_k(x) dA_x,$$

where  $\varepsilon_{ijk}$  is the standard permutation symbol. As before, when  $S$  is closed and bounded, we always choose  $n$  to be the outward unit normal field. In this case,  $F$  and  $T$  are loads exerted on  $S$  by the fluid exterior to  $S$ .

For convenience, we assume all quantities have been nondimensionalized using a characteristic length scale  $\ell > 0$ , a velocity scale  $\vartheta > 0$ , and a force scale  $\mu\vartheta\ell > 0$ , where  $\mu$  is the absolute viscosity of the fluid. The dimensional quantities corresponding to  $\{x, u, p, v\}$  are  $\{\ell x, \vartheta u, \mu\vartheta\ell^{-1}p, \vartheta v\}$ , and the dimensional quantities corresponding to  $\{Q, \sigma, f, F, T\}$  are  $\{\vartheta\ell^2 Q, \mu\vartheta\ell^{-1}\sigma, \mu\vartheta\ell^{-1}f, \mu\vartheta\ell F, \mu\vartheta\ell^2 T\}$ .

**3. Singular solutions of the Stokes equations.** In this section we outline various classic singular solutions of the homogeneous, free-space Stokes equations

$$(3.1) \quad \begin{aligned} u_{i,jj} - p_{,i} &= 0, & x \neq y, \\ u_{i,i} &= 0, & x \neq y, \\ u_i, p &\rightarrow 0, & |x| \rightarrow \infty. \end{aligned}$$

Here  $y$  is a given point called the pole of the solution. Various representations of the solution of (2.1) can be derived and understood in terms of these solutions and their properties. Notice that, by linearity, any multiple or linear combination of solutions of (3.1) is also a solution where defined. In what follows, we let  $z = x - y$  and  $r = |z|$ , and we let  $S_{\text{int}}$  and  $S_{\text{ext}}$  denote the interior and exterior domains associated with a given closed, bounded surface  $S$ . The notation and results outlined here will be employed throughout our developments.

**3.1. Point-source solution.** The point-source solution is defined by  $u_i = U_i^{\text{PS}}$ ,  $p = \Pi^{\text{PS}}$ ,  $\sigma_{ik} = \Xi_{ik}^{\text{PS}}$ , where

$$(3.2) \quad U_i^{\text{PS}} = \frac{z_i}{r^3}, \quad \Pi^{\text{PS}} = 0, \quad \Xi_{ik}^{\text{PS}} = \frac{2\delta_{ik}}{r^3} - \frac{6z_i z_k}{r^5}.$$

This solution may be derived from (3.1) by making the ansatz  $u_i = \phi_{,i}$  and  $p = 0$  for some radially symmetric function  $\phi$  [30]. The resultant force  $F$ , torque  $T$  about an arbitrary point  $c$ , and volume flow rate  $Q$  associated with an arbitrary closed, bounded surface  $S$  can be found by direct computation and depend on the relative location of the pole  $y$ . When  $y \in S_{\text{ext}}$  the divergence theorem and (3.1) can be used to show that the relevant integrals over  $S$  all vanish. When  $y \in S_{\text{int}}$  the divergence theorem and (3.1) can be used to transform the relevant integrals over  $S$  into integrals over an arbitrary sphere in  $S_{\text{int}}$  centered at  $y$ , which can then be evaluated directly. The results are

$$(3.3) \quad \begin{aligned} F_i &= 0, & T_i &= 0, & Q &= 4\pi, & y \in S_{\text{int}}, \\ F_i &= 0, & T_i &= 0, & Q &= 0, & y \in S_{\text{ext}}. \end{aligned}$$

**3.2. Point-source dipole solution.** The point-source dipole solution is defined by  $u_i = U_{ij}^{\text{PSD}} g_j$ ,  $p = \Pi_j^{\text{PSD}} g_j$ ,  $\sigma_{ik} = \Xi_{ikj}^{\text{PSD}} g_j$ , where  $g_j$  is an arbitrary vector independent of  $x$  and

$$(3.4) \quad \begin{aligned} U_{ij}^{\text{PSD}} &:= \frac{\partial}{\partial y_j} U_i^{\text{PS}} = -\frac{\delta_{ij}}{r^3} + \frac{3z_i z_j}{r^5}, & \Pi_j^{\text{PSD}} &:= \frac{\partial}{\partial y_j} \Pi^{\text{PS}} = 0, \\ \Xi_{ikj}^{\text{PSD}} &:= \frac{\partial}{\partial y_j} \Xi_{ik}^{\text{PS}} = \frac{6(\delta_{ik} z_j + \delta_{ij} z_k + \delta_{kj} z_i)}{r^5} - \frac{30z_i z_k z_j}{r^7}. \end{aligned}$$

This solution is implied by the solution in (3.2) and the linearity of (3.1). The resultant force  $F$ , torque  $T$  about an arbitrary point  $c$ , and volume flow rate  $Q$  associated with

an arbitrary closed, bounded surface  $S$  can be computed as previously described. The results are

$$(3.5) \quad \begin{aligned} F_i &= 0, & T_i &= 0, & Q &= 0, & y &\in S_{\text{int}}, \\ F_i &= 0, & T_i &= 0, & Q &= 0, & y &\in S_{\text{ext}}. \end{aligned}$$

**3.3. Point-force solution: Stokeslet.** The point-force solution is defined by  $u_i = U_{ij}^{\text{PF}} g_j$ ,  $p = \Pi_j^{\text{PF}} g_j$ ,  $\sigma_{ik} = \Xi_{ikj}^{\text{PF}} g_j$ , where  $g_j$  is an arbitrary vector independent of  $x$  and

$$(3.6) \quad U_{ij}^{\text{PF}} = \frac{\delta_{ij}}{r} + \frac{z_i z_j}{r^3}, \quad \Pi_j^{\text{PF}} = \frac{2z_j}{r^3}, \quad \Xi_{ikj}^{\text{PF}} = -\frac{6z_i z_k z_j}{r^5}.$$

Up to a normalizing constant, this solution corresponds to the classic fundamental solution of (3.1) and can be derived using the technique of Fourier transforms [20, 30]. It is typically referred to as a *stokeslet*. The resultant force  $F$ , torque  $T$  about an arbitrary point  $c$ , and volume flow rate  $Q$  associated with an arbitrary closed, bounded surface  $S$  can be computed as previously described. The results are

$$(3.7) \quad \begin{aligned} F_i &= -8\pi g_i, & T_i &= -8\pi \varepsilon_{ijk} (y_j - c_j) g_k, & Q &= 0, & y &\in S_{\text{int}}, \\ F_i &= 0, & T_i &= 0, & Q &= 0, & y &\in S_{\text{ext}}. \end{aligned}$$

**3.4. Point-force dipole solution: Stresslet, rotlet.** The point-force dipole solution is defined by  $u_i = U_{ijl}^{\text{PFD}} g_{jl}$ ,  $p = \Pi_{jl}^{\text{PFD}} g_{jl}$ ,  $\sigma_{ik} = \Xi_{ikjl}^{\text{PFD}} g_{jl}$ , where  $g_{jl}$  is an arbitrary tensor independent of  $x$  and

$$(3.8) \quad \begin{aligned} U_{ijl}^{\text{PFD}} &:= \frac{\partial}{\partial y_l} U_{ij}^{\text{PF}} = \frac{\delta_{ij} z_l - \delta_{il} z_j - \delta_{jl} z_i}{r^3} + \frac{3z_i z_j z_l}{r^5}, \\ \Pi_{jl}^{\text{PFD}} &:= \frac{\partial}{\partial y_l} \Pi_j^{\text{PF}} = -\frac{2\delta_{jl}}{r^3} + \frac{6z_j z_l}{r^5}, \\ \Xi_{ikjl}^{\text{PFD}} &:= \frac{\partial}{\partial y_l} \Xi_{ikj}^{\text{PF}} = \frac{6(\delta_{il} z_k z_j + \delta_{kl} z_i z_j + \delta_{jl} z_i z_k)}{r^5} - \frac{30z_i z_k z_j z_l}{r^7}. \end{aligned}$$

This solution is implied by the solution in (3.6) and the linearity of (3.1). By considering the decomposition  $g_{jl} = g_{jl}^{\text{sym}} + g_{jl}^{\text{skw}}$ , where  $g_{jl}^{\text{sym}} = \frac{1}{2}(g_{jl} + g_{lj})$  and  $g_{jl}^{\text{skw}} = \frac{1}{2}(g_{jl} - g_{lj})$ , and by using the parameterization  $g_{jl}^{\text{skw}} = \frac{1}{2} \varepsilon_{jml} g_m^{\text{vec}}$ , we find that the point-force dipole solution can be decomposed as

$$(3.9) \quad \begin{aligned} U_{ijl}^{\text{PFD}} g_{jl} &= -U_i^{\text{PS}} \delta_{jl} g_{jl}^{\text{sym}} + U_{ijl}^{\text{STR}} g_{jl}^{\text{sym}} + U_{im}^{\text{ROT}} g_m^{\text{vec}}, \\ \Pi_{jl}^{\text{PFD}} g_{jl} &= -\Pi^{\text{PS}} \delta_{jl} g_{jl}^{\text{sym}} + \Pi_{jl}^{\text{STR}} g_{jl}^{\text{sym}} + \Pi_m^{\text{ROT}} g_m^{\text{vec}}. \end{aligned}$$

Here  $(U_i^{\text{PS}}, \Pi^{\text{PS}})$  is the point-source solution given in (3.2) and  $(U_{ijl}^{\text{STR}}, \Pi_{jl}^{\text{STR}})$  and  $(U_{im}^{\text{ROT}}, \Pi_m^{\text{ROT}})$  are detailed below. By linearity, and the fact that  $g_{jl}^{\text{sym}}$  and  $g_m^{\text{vec}}$  are independent, we deduce that each of these pairs provides an independent solution of (3.1).

*Stresslet solution.* The stresslet solution is  $u_i = U_{ijl}^{\text{STR}} h_{jl}$ ,  $p = \Pi_{jl}^{\text{STR}} h_{jl}$ ,  $\sigma_{ik} = \Xi_{ikjl}^{\text{STR}} h_{jl}$ , where  $h_{jl}$  is an arbitrary tensor independent of  $x$  and

$$(3.10) \quad \begin{aligned} U_{ijl}^{\text{STR}} &= \frac{3z_i z_j z_l}{r^5}, & \Pi_{jl}^{\text{STR}} &= -\frac{2\delta_{jl}}{r^3} + \frac{6z_j z_l}{r^5}, \\ \Xi_{ikjl}^{\text{STR}} &= \frac{2\delta_{ik} \delta_{jl}}{r^3} + \frac{3(\delta_{ij} z_k z_l + \delta_{il} z_j z_k + \delta_{jk} z_i z_l + \delta_{lk} z_i z_j)}{r^5} - \frac{30z_i z_j z_k z_l}{r^7}. \end{aligned}$$

Due to the symmetry of the above functions in the indices  $j$  and  $l$  we notice that only the symmetric part of  $h_{jl}$  contributes to the solution in concordance with (3.9). The resultant force  $F$ , torque  $T$  about an arbitrary point  $c$ , and volume flow rate  $Q$  associated with an arbitrary closed, bounded surface  $S$  can be computed as previously described. The results are

$$(3.11) \quad \begin{aligned} F_i &= 0, & T_i &= 0, & Q &= 4\pi h_{jj}, & y &\in S_{\text{int}}, \\ F_i &= 0, & T_i &= 0, & Q &= 0, & y &\in S_{\text{ext}}. \end{aligned}$$

*Rotlet (or couplet) solution.* The rotlet solution is  $u_i = U_{ij}^{\text{ROT}} h_j$ ,  $p = \Pi_j^{\text{ROT}} h_j$ ,  $\sigma_{ik} = \Xi_{ikj}^{\text{ROT}} h_j$ , where  $h_j$  is an arbitrary vector independent of  $x$  and

$$(3.12) \quad U_{ij}^{\text{ROT}} = \frac{\varepsilon_{ijl} z_l}{r^3}, \quad \Pi_j^{\text{ROT}} = 0, \quad \Xi_{ikj}^{\text{ROT}} = \frac{3(\varepsilon_{ilj} z_k z_l + \varepsilon_{klj} z_i z_l)}{r^5}.$$

The resultant force  $F$ , torque  $T$  about an arbitrary point  $c$ , and volume flow rate  $Q$  associated with an arbitrary closed, bounded surface  $S$  can be computed as previously described. The results are

$$(3.13) \quad \begin{aligned} F_i &= 0, & T_i &= -8\pi h_i, & Q &= 0, & y &\in S_{\text{int}}, \\ F_i &= 0, & T_i &= 0, & Q &= 0, & y &\in S_{\text{ext}}. \end{aligned}$$

*Remarks 3.1.*

1. It can be shown that all higher-order point-source solutions beginning with the dipole can be expressed in terms of the point-force solution [30]. In particular, we have

$$U_{ij}^{\text{PSD}} = -\frac{1}{2} \frac{\partial^2 U_{ij}^{\text{PF}}}{\partial y_k \partial y_k}, \quad \Pi_j^{\text{PSD}} = -\frac{1}{2} \frac{\partial^2 \Pi_j^{\text{PF}}}{\partial y_k \partial y_k}.$$

Thus the family of higher-order point-source solutions is contained within the family of higher-order point-force solutions.

2. One approach to solving the boundary-value problem in (2.1) is to consider a linear combination (discrete or continuous) of singular solutions with poles placed arbitrarily within the body domain  $B$ . The coefficients in the combination are then determined by enforcing the boundary condition on  $\Gamma$ . However, because arbitrary boundary conditions can in general not be satisfied exactly in this approach, it yields only approximate solutions of (2.1) [7, 30]. For example, slender-body theory is based on this approach [4, 15, 17].
3. A related approach to solving (2.1) is to consider a linear combination of singular solutions with poles distributed continuously over the surface  $\Gamma$ . The density of the distribution is then determined by enforcing the boundary condition on  $\Gamma$ . This approach leads to the classic theory of surface potentials for the Stokes equations and yields exact representations of the solutions of (2.1) [20, 26, 29, 30].

**4. Surface potentials for the Stokes equations.** In this section we outline the classic single- and double-layer surface potentials for the Stokes equations and summarize their main properties. All the boundary integral formulations that we will study are based on these potentials. In what follows  $\Gamma$  is an arbitrary closed, bounded surface with interior domain  $B$  and exterior domain  $B_e$ , as described in section 2.

**4.1. Definition.** Let  $\psi : \Gamma \rightarrow \mathbb{R}^3$  be given. Then by the Stokes single-layer potentials on  $\Gamma$  with density  $\psi$  we mean

$$(4.1) \quad \begin{aligned} V_i[\Gamma, \psi](x) &= \int_{\Gamma} U_{ij}^{\text{PF}}(x, y) \psi_j(y) dA_y, \\ P_V[\Gamma, \psi](x) &= \int_{\Gamma} \Pi_j^{\text{PF}}(x, y) \psi_j(y) dA_y, \end{aligned}$$

and by the Stokes double-layer potentials on  $\Gamma$  with density  $\psi$  we mean

$$(4.2) \quad \begin{aligned} W_i[\Gamma, \psi](x) &= \int_{\Gamma} U_{ijl}^{\text{STR}}(x, y) \psi_j(y) \nu_l(y) dA_y, \\ P_W[\Gamma, \psi](x) &= \int_{\Gamma} \Pi_{jl}^{\text{STR}}(x, y) \psi_j(y) \nu_l(y) dA_y. \end{aligned}$$

Here  $(U_{ij}^{\text{PF}}, \Pi_j^{\text{PF}})$  is the point-force or stokeslet solution in (3.6) with pole at  $y$ ,  $(U_{ijl}^{\text{STR}}, \Pi_{jl}^{\text{STR}})$  is the stresslet solution in (3.10) with pole at  $y$ , and  $\nu$  is the unit normal field on  $\Gamma$  directed outwardly from  $B$ . All densities  $\psi$  will be assumed continuous.

**4.2. Analytic properties.** For arbitrary density  $\psi$  the single-layer potentials  $(V[\Gamma, \psi], P_V[\Gamma, \psi])$  and double-layer potentials  $(W[\Gamma, \psi], P_W[\Gamma, \psi])$  are smooth at each  $x \notin \Gamma$ . Moreover, by virtue of their definitions as continuous linear combinations of stokeslets and stresslets, they satisfy the homogeneous Stokes equations (2.1)<sub>1,2,4</sub> at each  $x \notin \Gamma$ .

For arbitrary  $\psi$  the functions  $V[\Gamma, \psi]$  and  $W[\Gamma, \psi]$  are well defined for all  $x \in B \cup \Gamma \cup B_e$ . For  $x \in \Gamma$  the integrands in (4.1)<sub>1</sub> and (4.2)<sub>1</sub> are unbounded functions of  $y \in \Gamma$ , but the integrals exist as improper integrals in the usual sense [13] provided that  $\Gamma$  is a Lyapunov surface. The restrictions of  $V[\psi, \Gamma]$  and  $W[\psi, \Gamma]$  to  $\Gamma$  are denoted by  $\overline{V}[\psi, \Gamma]$  and  $\overline{W}[\psi, \Gamma]$ . These restrictions are continuous functions on  $\Gamma$  [20]. Moreover, for any  $x_0 \in \Gamma$  the following limit relations hold [20, 29, 30]:

$$(4.3) \quad \lim_{\substack{x \rightarrow x_0 \\ x \in B_e}} V[\Gamma, \psi](x) = \overline{V}[\Gamma, \psi](x_0),$$

$$(4.4) \quad \lim_{\substack{x \rightarrow x_0 \\ x \in B}} V[\Gamma, \psi](x) = \overline{V}[\Gamma, \psi](x_0),$$

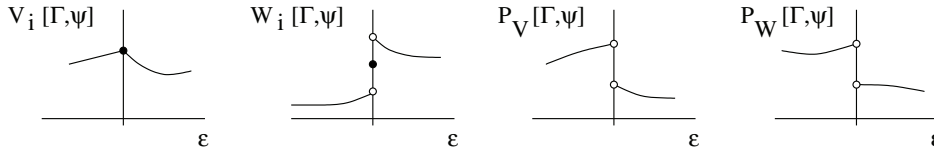
$$(4.5) \quad \lim_{\substack{x \rightarrow x_0 \\ x \in B_e}} W[\Gamma, \psi](x) = \alpha \psi(x_0) + \overline{W}[\Gamma, \psi](x_0),$$

$$(4.6) \quad \lim_{\substack{x \rightarrow x_0 \\ x \in B}} W[\Gamma, \psi](x) = -\alpha \psi(x_0) + \overline{W}[\Gamma, \psi](x_0).$$

Here  $\alpha$  is a constant that depends on the choice of normalization of the stresslet solution (3.10). For our choice we have  $\alpha = 2\pi$ . Notice that, by continuity of  $\psi$  and  $\overline{W}[\Gamma, \psi]$ , the one-sided limits in (4.5) and (4.6) are themselves continuous functions on  $\Gamma$ .

In contrast to the case with  $V[\Gamma, \psi]$  and  $W[\Gamma, \psi]$ , for arbitrary  $\psi$  the functions  $P_V[\Gamma, \psi]$  and  $P_W[\Gamma, \psi]$  do not exist as improper integrals in the usual sense when  $x \in \Gamma$ . In particular, the integrands in (4.1)<sub>2</sub> and (4.2)<sub>2</sub> are excessively singular functions of  $y \in \Gamma$ . Nevertheless, for sufficiently smooth  $\Gamma$  and  $\psi$ , the functions  $P_V[\Gamma, \psi]$  and  $P_W[\Gamma, \psi]$  have well-defined limits as  $x$  approaches the surface  $\Gamma$  [20, 29, 33]. Introducing  $x_\epsilon = x_0 + \epsilon \nu(x_0)$ , where  $x_0 \in \Gamma$ , the continuity properties of

the functions  $V[\Gamma, \psi]$ ,  $W[\Gamma, \psi]$ ,  $P_V[\Gamma, \psi]$ ,  $P_W[\Gamma, \psi]$  around  $\epsilon = 0$  can be illustrated as follows:



In general, the limits of the functions  $V[\Gamma, \psi]$ ,  $W[\Gamma, \psi]$ ,  $P_V[\Gamma, \psi]$ ,  $P_W[\Gamma, \psi]$  as  $x$  approaches  $\Gamma$  from  $B_\epsilon$  or  $B$  have more physical significance than any directly defined values of these functions on  $\Gamma$ . In particular, physically meaningful boundary conditions are imposed on limit values and not on directly defined values. We remark that directly defined values of  $P_V[\Gamma, \psi]$  and  $P_W[\Gamma, \psi]$  on  $\Gamma$  may be obtained by appealing to the theory of singular and hypersingular integrals [22, 24, 25].

**4.3. Associated stress fields.** For arbitrary  $\psi$  the stress fields associated with the single- and double-layer potentials are

$$(4.7) \quad \Sigma_V^{ik}[\Gamma, \psi](x) = \int_\Gamma \Xi_{ikj}^{PF}(x, y)\psi_j(y) dA_y,$$

$$(4.8) \quad \Sigma_W^{ik}[\Gamma, \psi](x) = \int_\Gamma \Xi_{ikjl}^{STR}(x, y)\psi_j(y)\nu_l(y) dA_y,$$

where  $\Xi_{ikj}^{PF}$  and  $\Xi_{ikjl}^{STR}$  are the stress functions corresponding to the point-force and stresslet solutions in (3.6) and (3.10). For arbitrary  $\psi$  the single-layer stress field  $\Sigma_V[\Gamma, \psi]$  is smooth at each  $x \notin \Gamma$  and is the actual stress field associated with the Stokes flow with velocity field  $V[\Gamma, \psi]$  and pressure field  $P_V[\Gamma, \psi]$ . A similar remark applies to the double-layer stress field  $\Sigma_W[\Gamma, \psi]$ .

For  $x \in \Gamma$  and arbitrary  $\psi$  the single-layer traction field  $\Sigma_V[\Gamma, \psi]\nu$  exists as an improper integral in the usual sense—but not the double-layer traction field  $\Sigma_W[\Gamma, \psi]\nu$ . Moreover, for sufficiently smooth  $\Gamma$  and  $\psi$  the following limit relations for  $\Sigma_V[\Gamma, \psi]\nu$  [20, 29] and  $\Sigma_W[\Gamma, \psi]\nu$  [29] hold for each  $x_0 \in \Gamma$ :

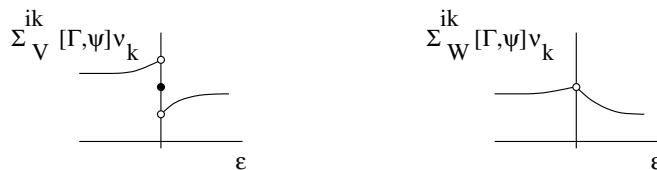
$$(4.9) \quad \lim_{\substack{\epsilon \rightarrow 0 \\ \epsilon > 0}} \Sigma_V[\Gamma, \psi](x_\epsilon)\nu(x_0) = \beta\psi(x_0) + \Sigma_V[\Gamma, \psi](x_0)\nu(x_0),$$

$$(4.10) \quad \lim_{\substack{\epsilon \rightarrow 0 \\ \epsilon < 0}} \Sigma_V[\Gamma, \psi](x_\epsilon)\nu(x_0) = -\beta\psi(x_0) + \Sigma_V[\Gamma, \psi](x_0)\nu(x_0),$$

$$(4.11) \quad \lim_{\substack{\epsilon \rightarrow 0 \\ \epsilon > 0}} \Sigma_W[\Gamma, \psi](x_\epsilon)\nu(x_0) = \lim_{\substack{\epsilon \rightarrow 0 \\ \epsilon < 0}} \Sigma_W[\Gamma, \psi](x_\epsilon)\nu(x_0).$$

Here  $x_\epsilon = x_0 + \epsilon\nu(x_0)$  and  $\beta$  is a constant that depends on the choice of normalization of the point-force solution (3.6). For our choice we have  $\beta = -4\pi$ . The result in (4.11) is commonly referred to as the Lyapunov–Tauber condition.

For arbitrary  $\psi$  and  $x_0 \in \Gamma$  the continuity properties of  $\Sigma_V[\Gamma, \psi](x_\epsilon)\nu(x_0)$  and  $\Sigma_W[\Gamma, \psi](x_\epsilon)\nu(x_0)$  around  $\epsilon = 0$  can be illustrated as follows:





We remark that, as with  $P_W[\Gamma, \psi]$ , a directly defined value of  $\Sigma_W[\Gamma, \psi]\nu$  on  $\Gamma$  may be obtained by appealing to the theory of hypersingular integrals.

**4.4. Flow properties.** Let  $S$  be an arbitrary closed, bounded surface with  $\Gamma \subset S_{\text{int}}$ , and let  $n$  be the outward unit normal field on  $S$ . For arbitrary  $\psi$  the resultant force  $F_V[\Gamma, \psi]$ , torque  $T_V[\Gamma, \psi]$  about an arbitrary point  $c$ , and volume flow rate  $Q_V[\Gamma, \psi]$  associated with  $S$  and the single-layer flow  $(V[\Gamma, \psi], P_V[\Gamma, \psi])$  are

$$(4.12) \quad F_V[\Gamma, \psi] = \int_S \Sigma_V[\Gamma, \psi](x)n(x) dA_x = -8\pi \int_{\Gamma} \psi(y) dA_y,$$

$$(4.13) \quad T_V[\Gamma, \psi] = \int_S (x - c) \times \Sigma_V[\Gamma, \psi](x)n(x) dA_x = -8\pi \int_{\Gamma} (y - c) \times \psi(y) dA_y,$$

$$(4.14) \quad Q_V[\Gamma, \psi] = \int_S V[\Gamma, \psi](x) \cdot n(x) dA_x = 0.$$

These results follow from the definitions of the single-layer stress and velocity fields in (4.7) and (4.1) and the properties of the point-force solution in (3.6) and (3.7) with  $g_i$  replaced by  $\psi_i$ . Because the above results are independent of  $S$  with  $\Gamma \subset S_{\text{int}}$ , we can pass to the limit and conclude that the resultant force, torque, and volume flow rate associated with  $\Gamma$  and the exterior single-layer flow are also given by the above results.

Similar calculations can be performed in the double-layer case. For arbitrary  $\psi$  the resultant force  $F_W[\Gamma, \psi]$ , torque  $T_W[\Gamma, \psi]$  about an arbitrary point  $c$ , and volume flow rate  $Q_W[\Gamma, \psi]$  associated with  $S$  and the double-layer flow  $(W[\Gamma, \psi], P_W[\Gamma, \psi])$  are

$$(4.15) \quad F_W[\Gamma, \psi] = \int_S \Sigma_W[\Gamma, \psi](x)n(x) dA_x = 0,$$

$$(4.16) \quad T_W[\Gamma, \psi] = \int_S (x - c) \times \Sigma_W[\Gamma, \psi](x)n(x) dA_x = 0,$$

$$(4.17) \quad Q_W[\Gamma, \psi] = \int_S W[\Gamma, \psi](x) \cdot n(x) dA_x = 4\pi \int_{\Gamma} \psi(y) \cdot \nu(y) dA_y.$$

These results follow from the definitions of the double-layer stress and velocity fields in (4.8) and (4.2) and the properties of the stresslet solution in (3.10) and (3.11) with  $h_{jl}$  replaced by  $\psi_j \nu_l$ . As before, because the above results are independent of  $S$  with  $\Gamma \subset S_{\text{int}}$ , we can pass to the limit and conclude that the resultant force, torque, and volume flow rate associated with  $\Gamma$  and the exterior double-layer flow are also given by the above results.

**5. Hebeker formulation.** In this section we outline the boundary integral formulation of (2.1) introduced by Hebeker [14] and highlight several of its properties for comparison. In what follows  $\Gamma$  is an arbitrary closed, bounded surface with interior domain  $B$  and exterior domain  $B_e$ , as described in section 2.

**5.1. Formulation.** Given an arbitrary density  $\psi : \Gamma \rightarrow \mathbb{R}^3$  and number  $\theta \in [0, 1]$ , define  $u : B_e \rightarrow \mathbb{R}^3$  and  $p : B_e \rightarrow \mathbb{R}$  by

$$(5.1) \quad u = \theta V[\Gamma, \psi] + (1 - \theta)W[\Gamma, \psi], \quad p = \theta P_V[\Gamma, \psi] + (1 - \theta)P_W[\Gamma, \psi].$$

By properties of the single- and double-layer potentials, the fields  $(u, p)$  are smooth at each  $x \in B_e$  and satisfy the Stokes equations (2.1)<sub>1,2,4</sub> at each  $x \in B_e$ . The stress

field  $\sigma : B_e \rightarrow \mathbb{R}^{3 \times 3}$  associated with  $(u, p)$  is given by

$$(5.2) \quad \sigma = \theta \Sigma_V[\Gamma, \psi] + (1 - \theta) \Sigma_W[\Gamma, \psi],$$

and the resultant force  $F$ , torque  $T$  about an arbitrary point  $c$ , and volume flow rate  $Q$  associated with  $\Gamma$  are

$$(5.3) \quad F = \theta F_V[\Gamma, \psi], \quad T = \theta T_V[\Gamma, \psi], \quad Q = (1 - \theta) Q_W[\Gamma, \psi].$$

Here we have used linearity and the flow properties of the single- and double-layer potentials outlined in section 4.4.

In order for  $(u, p)$  to provide the unique solution of the exterior Stokes boundary-value problem (2.1), the boundary condition (2.1)<sub>3</sub> must be satisfied. In particular, given  $v : \Gamma \rightarrow \mathbb{R}^3$ , we require

$$(5.4) \quad \lim_{\substack{x \rightarrow x_0 \\ x \in B_e}} u(x) = v(x_0) \quad \forall x_0 \in \Gamma.$$

Substituting for  $u$  from (5.1) and using the limit relations in (4.3) and (4.5), we obtain a boundary integral equation for the unknown density  $\psi$ :

$$(5.5) \quad \theta \overline{V}[\Gamma, \psi](x_0) + (1 - \theta) \overline{W}[\Gamma, \psi](x_0) + (1 - \theta) \alpha \psi(x_0) = v(x_0) \quad \forall x_0 \in \Gamma.$$

From this we can deduce that  $(u, p)$  defined in (5.1) will be the unique solution of (2.1) if and only if  $\psi$  satisfies (5.5). This equation can be written in the standard form

$$(5.6) \quad \int_{\Gamma} K_{\theta}(x, y) \psi(y) dA_y + c_{\theta} \psi(x) = v(x) \quad \forall x \in \Gamma,$$

where  $x_0$  has been replaced by  $x$  for convenience,  $c_{\theta} = (1 - \theta) \alpha$ , and

$$(5.7) \quad K_{\theta}^{ij}(x, y) = \theta U_{ij}^{\text{PF}}(x, y) + (1 - \theta) U_{ijl}^{\text{STR}}(x, y) \nu_l(y).$$

*Remarks 5.1.*

1. Assuming  $\Gamma$  is a Lyapunov surface the kernel function  $K_{\theta}(x, y)$  can be shown to be weakly singular. Thus the solvability of the linear integral equation (5.6) can be assessed via the Fredholm theory [19, 23]. Notice that  $c_{\theta} = 0$  when  $\theta = 1$ , and  $c_{\theta} \neq 0$  when  $\theta \in [0, 1)$ . Thus (5.6) is a Fredholm equation of the first kind when  $\theta = 1$  and of the second kind when  $\theta \in [0, 1)$ .
2. The case  $\theta = 0$  in (5.1) corresponds to a classic double-layer representation of  $(u, p)$ . It is well known that this representation is incomplete in the sense that it can represent only those flows for which the resultant force and torque on  $\Gamma$  vanish, that is,  $F = 0$  and  $T = 0$  [20, 26, 29, 30]. Equivalently, the range of the linear operator in (5.6) is deficient, leading to solvability conditions and nonuniqueness for  $\psi$ .
3. The case  $\theta = 1$  in (5.1) corresponds to a classic single-layer representation of  $(u, p)$ . It is well known that this representation is also incomplete in the sense that it can represent only those flows for which the volumetric expansion rate of  $\Gamma$  vanishes, that is,  $Q = 0$  [20, 26, 29, 30]. Equivalently, the range of the linear operator in (5.6) is again deficient, leading to solvability conditions and nonuniqueness for  $\psi$ .

4. The main idea in Hebeker [14] was to consider a mixed representation corresponding to  $\theta \in (0, 1)$ . The intuitive motivation is that, by considering a linear combination, each potential can make up for the deficiencies of the other. As outlined below, such a representation is complete in the sense that it can represent arbitrary flows and stable in the sense that the density  $\psi$  depends continuously on the boundary data  $v$ .

**5.2. Solvability result.** The following is a slight generalization of the solvability result given in Hebeker [14].

**THEOREM 5.1** (see [14]). *Assume  $\Gamma$  is a closed, bounded Lyapunov surface. If  $\theta \in (0, 1)$ , then (5.6) possesses a unique continuous solution  $\psi$  for any continuous boundary data  $v$ .*

Thus arbitrary solutions of the exterior Stokes boundary-value problem (2.1) can be represented in the form (5.1) with a unique density  $\psi$  for each  $\theta \in (0, 1)$ . The presence of the double-layer potential in (5.1) ensures that the representation is stable. In particular, because (5.6) is a uniquely solvable Fredholm equation of the second kind, the linear operator in (5.6) has a finite condition number and the density  $\psi$  depends continuously on the data  $v$ . The presence of the single-layer potential in (5.1) ensures that the representation is complete. In particular, the single-layer potential completes the deficient range associated with the double-layer potential. The smoothness properties of the density  $\psi$  depend on those of the surface  $\Gamma$  and the data  $v$ .

*Remarks 5.2.*

1. Aside from the restriction of solvability, the parameter  $\theta$  is arbitrary and can be exploited. For example,  $\theta \in (0, 1)$  might be chosen by some means to optimize the conditioning of the linear operator in (5.6).
2. Numerical methods for (5.6), Nyström methods in particular, must deal with the singularities in the kernels of the single- and double-layer potentials. The singularity in the kernel of the double-layer potential can be removed in a simple, standard way by employing a well-known integral identity [11, 28, 30, 31] (see section 8). However, there seems to be no similar removal technique for the singularity in the kernel of the single-layer potential.
3. In general numerical treatments, the singularity in the kernel of the single-layer potential can be dealt with by employing a kernel-adapted product quadrature rule [3, 19], together with a local coordinate transformation such as a Duffy transformation [3, 8, 30], or a floating polar transformation [33]. The same techniques can also be applied to the double-layer potential. In view of the inconvenience associated with the single-layer potential, we investigate alternative formulations.

**6. Power and Miranda formulation.** In this section we outline the boundary integral formulation of (2.1) introduced by Power and Miranda [28] and highlight several of its properties for comparison. In what follows  $\Gamma$  is an arbitrary closed, bounded surface with interior domain  $B$  and exterior domain  $B_e$ , as described in section 2. For simplicity, in this section we assume that  $B$  consists of only one connected component. All the results outlined generalize in a straightforward way to the case when  $B$  has a finite number of disjoint components [29].

**6.1. Formulation.** Given an arbitrary density  $\psi : \Gamma \rightarrow \mathbb{R}^3$ , number  $\theta \in [0, 1]$ , and point  $x_* \in B$ , define  $u : B_e \rightarrow \mathbb{R}^3$  and  $p : B_e \rightarrow \mathbb{R}$  by

$$(6.1) \quad u = \theta Y[\Gamma, \psi] + (1 - \theta)W[\Gamma, \psi], \quad p = \theta P_Y[\Gamma, \psi] + (1 - \theta)P_W[\Gamma, \psi],$$

where  $Y[\Gamma, \psi]$  and  $P_Y[\Gamma, \psi]$  are fields defined in terms of the point-force (stokeslet) and rotlet solutions as

$$(6.2) \quad \begin{aligned} Y_i[\Gamma, \psi](x) &= \int_{\Gamma} \left( U_{ij}^{\text{PF}}(x, x_*) + U_{il}^{\text{ROT}}(x, x_*) \varepsilon_{lpj} (y_p - x_{*p}) \right) \psi_j(y) dA_y, \\ P_Y[\Gamma, \psi](x) &= \int_{\Gamma} \left( \Pi_j^{\text{PF}}(x, x_*) + \Pi_l^{\text{ROT}}(x, x_*) \varepsilon_{lpj} (y_p - x_{*p}) \right) \psi_j(y) dA_y. \end{aligned}$$

By properties of the point-force and rotlet solutions and the double-layer potentials, the fields  $(u, p)$  are smooth at each  $x \in B_e$  and satisfy the Stokes equations (2.1)<sub>1,2,4</sub> at each  $x \in B_e$ . The stress field  $\sigma : B_e \rightarrow \mathbb{R}^{3 \times 3}$  associated with  $(u, p)$  is given by

$$(6.3) \quad \sigma = \theta \Sigma_Y[\Gamma, \psi] + (1 - \theta) \Sigma_W[\Gamma, \psi],$$

where  $\Sigma_Y[\Gamma, \psi]$  is the stress field associated with the flow  $(Y[\Gamma, \psi], P_Y[\Gamma, \psi])$ , namely,

$$(6.4) \quad \Sigma_Y^{ik}[\Gamma, \psi](x) = \int_{\Gamma} \left( \Xi_{ikj}^{\text{PF}}(x, x_*) + \Xi_{ikl}^{\text{ROT}}(x, x_*) \varepsilon_{lpj} (y_p - x_{*p}) \right) \psi_j(y) dA_y.$$

The resultant force  $F$ , torque  $T$  about an arbitrary point  $c$ , and volume flow rate  $Q$  associated with  $\Gamma$  are

$$(6.5) \quad F = \theta F_Y[\Gamma, \psi], \quad T = \theta T_Y[\Gamma, \psi], \quad Q = \theta Q_Y[\Gamma, \psi] + (1 - \theta) Q_W[\Gamma, \psi],$$

where  $F_Y[\Gamma, \psi]$ ,  $T_Y[\Gamma, \psi]$ , and  $Q_Y[\Gamma, \psi]$  are the resultant force, torque, and volume flow rate associated with the flow  $(Y[\Gamma, \psi], P_Y[\Gamma, \psi])$ . From the properties of the point-force and rotlet solutions given in (3.7) and (3.13), we deduce that  $Q_Y[\Gamma, \psi] = 0$  and

$$(6.6) \quad F_Y[\Gamma, \psi] = -8\pi \int_{\Gamma} \psi(y) dA_y, \quad T_Y[\Gamma, \psi] = -8\pi \int_{\Gamma} (y - c) \times \psi(y) dA_y.$$

In order for  $(u, p)$  to provide the unique solution of the exterior Stokes boundary-value problem (2.1), the boundary condition (2.1)<sub>3</sub> must be satisfied. In particular, given  $v : \Gamma \rightarrow \mathbb{R}^3$ , we require

$$(6.7) \quad \lim_{\substack{x \rightarrow x_0 \\ x \in B_e}} u(x) = v(x_0) \quad \forall x_0 \in \Gamma.$$

Substituting for  $u$  from (6.1) and using the limit relation in (4.5), we obtain a boundary integral equation for the unknown density  $\psi$ :

$$(6.8) \quad \theta Y[\Gamma, \psi](x_0) + (1 - \theta) \overline{W}[\Gamma, \psi](x_0) + (1 - \theta) \alpha \psi(x_0) = v(x_0) \quad \forall x_0 \in \Gamma.$$

From this we can deduce that  $(u, p)$  defined in (6.1) will be the unique solution of (2.1) if and only if  $\psi$  satisfies (6.8). This equation can be written in the standard form

$$(6.9) \quad \int_{\Gamma} K_{\theta}(x, y) \psi(y) dA_y + c_{\theta} \psi(x) = v(x) \quad \forall x \in \Gamma,$$

where  $x_0$  has been replaced by  $x$  for convenience,  $c_{\theta} = (1 - \theta) \alpha$ , and

$$(6.10) \quad \begin{aligned} K_{\theta}^{ij}(x, y) &= \theta U_{ij}^{\text{PF}}(x, x_*) + \theta U_{il}^{\text{ROT}}(x, x_*) \varepsilon_{lpj} (y_p - x_{*p}) \\ &\quad + (1 - \theta) U_{ijl}^{\text{STR}}(x, y) \nu_l(y). \end{aligned}$$

*Remarks 6.1.*

1. As before, assuming  $\Gamma$  is a Lyapunov surface, the kernel function  $K_\theta(x, y)$  can be shown to be weakly singular. Thus the solvability of the linear integral equation (6.9) can be assessed via the Fredholm theory [19, 23]. Notice that  $c_\theta = 0$  when  $\theta = 1$ , and  $c_\theta \neq 0$  when  $\theta \in [0, 1)$ . Thus (6.9) is a Fredholm equation of the first kind when  $\theta = 1$  and of the second kind when  $\theta \in [0, 1)$ .
2. The main idea in Power and Miranda [28] can be described intuitively as follows. A double-layer potential is deficient in the sense that it can only produce flows with zero resultant force and torque on  $\Gamma$ . Thus, in view of the flow properties outlined in (3.7) and (3.13), the enhancement of a double-layer potential with point-force and rotlet solutions should produce flows with arbitrary resultant force and torque on  $\Gamma$ .
3. The intuitive arguments above are made rigorous by the results outlined below. They show that the representation in (6.1) with  $\theta \in (0, 1)$  is complete in the sense that it can represent arbitrary flows and stable in the sense that the density  $\psi$  depends continuously on the boundary data  $v$ .

**6.2. Solvability result.** The following is a slight generalization of the solvability result given in Power and Miranda [28].

**THEOREM 6.1** (see [28]). *Assume  $\Gamma$  is a closed, bounded Lyapunov surface, and let  $x_* \in B$  be arbitrary. If  $\theta \in (0, 1)$ , then (6.9) possesses a unique continuous solution  $\psi$  for any continuous boundary data  $v$ .*

Thus arbitrary solutions of the exterior Stokes boundary-value problem (2.1) can be represented in the form (6.1) with a unique density  $\psi$  for each  $x_* \in B$  and  $\theta \in (0, 1)$ . The presence of the double-layer potential in (6.1) ensures that the representation is stable. In particular, because (6.9) is a uniquely solvable Fredholm equation of the second kind, the linear operator in (6.9) has a finite condition number and the density  $\psi$  depends continuously on the data  $v$ . The presence of the point-force and rotlet functions in (6.1) ensures that the representation is complete. In particular, these two singular solutions complete the deficient range associated with the double-layer potential. The smoothness properties of the density  $\psi$  depend on those of the surface  $\Gamma$  and the data  $v$ .

*Remarks 6.2.*

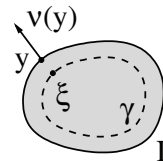
1. Aside from the restriction of solvability, the parameters  $\theta$  and  $x_*$  are arbitrary and can be exploited. For example,  $\theta \in (0, 1)$  and  $x_* \in B$  might be chosen by some means to optimize the conditioning of the linear operator in (6.9).
2. The boundary integral equation in (6.9) can be described as being singularity-free. The singularity in the point-force and rotlet contributions is avoided because their poles are contained in the body domain  $B$ . Moreover, the singularity in the kernel of the double-layer potential can be removed in a simple, standard way by employing a well-known integral identity [11, 28, 30, 31] (see section 8).
3. The above results hold for bodies of arbitrary shape. For certain types of bodies, for example convex or star-shaped bodies, there are various reasonable choices for the point  $x_* \in B$ . The center of volume is one obvious choice. In contrast, for other types of bodies, for example, toroidal or knotted tubular bodies, there seems to be no natural choice for the point  $x_* \in B$ . Motivated by this latter class of bodies, we investigate an alternative formulation.

**7. A new formulation.** Here we introduce a new boundary integral formulation of (2.1) which combines the strengths of the Power and Miranda and the Hebecker

formulations. The new formulation is stable, complete, singularity-free, and natural for bodies of complicated shape and topology. In what follows  $\Gamma$  is an arbitrary closed, bounded surface with interior domain  $B$  and exterior domain  $B_e$ , as described in section 2.

**7.1. Formulation.** Let  $\gamma$  be a surface parallel to  $\Gamma$  offset toward  $B$  by a distance  $\phi \geq 0$ . In particular,  $\gamma$  is the image of the map  $\xi = \zeta(y) : \Gamma \rightarrow \mathbb{R}^3$  defined by

(7.1)



$$\xi = y - \phi \nu(y).$$

By virtue of the fact that  $\Gamma$  is a Lyapunov surface, it follows that the map  $\zeta : \Gamma \rightarrow \gamma$  is continuous and one-to-one for all  $\phi \in [0, \phi_\Gamma]$ , where  $\phi_\Gamma$  is a positive constant. In the absence of any global obstructions, we have  $\phi_\Gamma = 1/\kappa_\Gamma$ , where  $\kappa_\Gamma$  is the maximum of the signed principal curvatures of  $\Gamma$  [27]. Here we use the convention that the curvature is positive when  $\Gamma$  curves away from its outward unit normal  $\nu$ . As a consequence, the principal curvatures are the eigenvalues of the gradient of  $\nu$  (not  $-\nu$ ) restricted to the tangent plane. From the geometry of parallel surfaces we have the following relations for all  $y \in \Gamma$ ,  $\xi = \zeta(y) \in \gamma$ , and  $\phi \in [0, \phi_\Gamma]$  [27]:

$$(7.2) \quad n(\xi) = \nu(y), \quad dA_\xi = J^\phi(y) dA_y, \quad J^\phi(y) = 1 - 2\phi\kappa^m(y) + \phi^2\kappa^g(y).$$

Here  $n$  is the outward unit normal on  $\gamma$ ,  $dA_\xi$  and  $dA_y$  are area elements on  $\gamma$  and  $\Gamma$ , and  $\kappa^m$  and  $\kappa^g$  are the mean and Gaussian curvatures of  $\Gamma$ . For  $\phi \in [0, \phi_\Gamma]$  we denote the inverse of  $\xi = \zeta(y)$  by  $y = \varphi(\xi)$ . In view of (7.1) and (7.2)<sub>1</sub> we have  $y = \xi + \phi n(\xi)$ .

Given an arbitrary density  $\psi : \Gamma \rightarrow \mathbb{R}^3$  and number  $\theta \in [0, 1]$ , define  $u : B_e \rightarrow \mathbb{R}^3$  and  $p : B_e \rightarrow \mathbb{R}$  by

$$(7.3) \quad u = \theta V[\gamma, \psi \circ \varphi] + (1 - \theta)W[\Gamma, \psi], \quad p = \theta P_V[\gamma, \psi \circ \varphi] + (1 - \theta)P_W[\Gamma, \psi].$$

Notice that the double-layer potentials are defined on the surface  $\Gamma$  with density  $\psi$ , while the single-layer potentials are defined on the parallel surface  $\gamma$  with density  $\psi \circ \varphi$ . In particular, the two types of potentials are defined on different surfaces but involve only one arbitrary density.

By properties of the single- and double-layer potentials, the fields  $(u, p)$  are smooth at each  $x \in B_e$  and satisfy the Stokes equations (2.1)<sub>1,2,4</sub> at each  $x \in B_e$ . The stress field  $\sigma : B_e \rightarrow \mathbb{R}^{3 \times 3}$  associated with  $(u, p)$  is given by

$$(7.4) \quad \sigma = \theta \Sigma_V[\gamma, \psi \circ \varphi] + (1 - \theta) \Sigma_W[\Gamma, \psi],$$

and the resultant force  $F$ , torque  $T$  about an arbitrary point  $c$ , and volume flow rate  $Q$  associated with  $\Gamma$  are

$$(7.5) \quad F = \theta F_V[\gamma, \psi \circ \varphi], \quad T = \theta T_V[\gamma, \psi \circ \varphi], \quad Q = (1 - \theta)Q_W[\Gamma, \psi].$$

Here we have used linearity and the flow properties of the single- and double-layer potentials outlined in section 4.4.

In order for  $(u, p)$  to provide the unique solution of the exterior Stokes boundary-value problem (2.1), the boundary condition (2.1)<sub>3</sub> must be satisfied. In particular, given  $v : \Gamma \rightarrow \mathbb{R}^3$ , we require

$$(7.6) \quad \lim_{\substack{x \rightarrow x_0 \\ x \in B_e}} u(x) = v(x_0) \quad \forall x_0 \in \Gamma.$$

Substituting for  $u$  from (7.3) and using the limit relation in (4.5), we obtain a boundary integral equation for the unknown density  $\psi$ :

$$(7.7) \quad \theta V[\gamma, \psi \circ \varphi](x_0) + (1 - \theta)\overline{W}[\Gamma, \psi](x_0) + (1 - \theta)\alpha\psi(x_0) = v(x_0) \quad \forall x_0 \in \Gamma.$$

From this we can deduce that  $(u, p)$  defined in (7.3) will be the unique solution of (2.1) if and only if  $\psi$  satisfies (7.7). By definition of the single- and double-layer potentials, this equation can be written in integral form as

$$(7.8) \quad \theta \int_{\gamma} U_{ij}^{PF}(x, \xi)\psi_j(\varphi(\xi)) dA_{\xi} + (1 - \theta) \int_{\Gamma} U_{ijl}^{STR}(x, y)\psi_j(y)\nu_l(y) dA_y + c_{\theta}\psi_i(x) = v_i(x) \quad \forall x \in \Gamma,$$

where  $x_0$  has been replaced by  $x$  for convenience and  $c_{\theta} = (1 - \theta)\alpha$ . By performing a change of variable in the first integral, this equation can then be put into the standard form

$$(7.9) \quad \int_{\Gamma} K_{\theta}(x, y)\psi(y) dA_y + c_{\theta}\psi(x) = v(x) \quad \forall x \in \Gamma,$$

where

$$(7.10) \quad K_{\theta}^{ij}(x, y) = \theta J^{\phi}(y)U_{ij}^{PF}(x, \zeta(y)) + (1 - \theta)U_{ijl}^{STR}(x, y)\nu_l(y).$$

*Remarks 7.1.*

1. In all three formulations the kernel function  $K_{\theta}(x, y)$  can be described as the positive linear combination of a double-layer kernel and a range completion term. In the Hebeker formulation (5.7), the completion term is an unbounded single-layer kernel. In the Power and Miranda formulation (6.10), the completion term is the sum of a point-force and a rotlet kernel, both of which are bounded and dependent on a point  $x_* \in B$ . In the new formulation (7.10), the completion term can be interpreted as a regularized single-layer kernel, where  $\phi \geq 0$  is the regularization parameter. The regularized single-layer kernel is bounded when  $\phi > 0$  and unbounded exactly as in the Hebeker formulation when  $\phi = 0$ .
2. Assuming  $\Gamma$  is a Lyapunov surface, the kernel function  $K_{\theta}(x, y)$  in (7.10) can be shown to be weakly singular. Thus the solvability of the linear integral equation (7.9) can be assessed via the Fredholm theory [19, 23]. Notice that  $c_{\theta} = 0$  when  $\theta = 1$  and  $c_{\theta} \neq 0$  when  $\theta \in [0, 1)$ . Thus (7.9) is a Fredholm equation of the first kind when  $\theta = 1$  and of the second kind when  $\theta \in [0, 1)$ .
3. As outlined below, the representation in (7.3) with  $\theta \in (0, 1)$  is complete in the sense that it can represent arbitrary flows and stable in the sense that the density  $\psi$  depends continuously on the boundary data  $v$ .

**7.2. Solvability result.** The following result establishes the solvability of the integral equation (7.9), or, equivalently, (7.7). Its proof is given in section 7.3 below.

**THEOREM 7.1.** *Assume  $\Gamma$  is a closed, bounded Lyapunov surface, and let  $\gamma$  be a surface parallel to  $\Gamma$  offset toward  $B$  by a distance  $\phi \in [0, \phi_{\Gamma})$ . If  $\theta \in (0, 1)$ , then (7.9) possesses a unique continuous solution  $\psi$  for any continuous boundary data  $v$ .*

Thus arbitrary solutions of the exterior Stokes boundary-value problem (2.1) can be represented in the form (7.3) with a unique density  $\psi$  for each  $\theta \in (0, 1)$  and

$\phi \in [0, \phi_\Gamma]$ . The presence of the double-layer potential in (7.3) ensures that the representation is stable. In particular, because (7.9) is a uniquely solvable Fredholm equation of the second kind, the linear operator in (7.9) has a finite condition number, and the density  $\psi$  depends continuously on the data  $v$ . The presence of the single-layer potential in (7.3) ensures that the representation is complete. In particular, the single-layer potential on the parallel surface  $\gamma$  completes the deficient range associated with the double-layer potential on the surface  $\Gamma$ . The smoothness properties of the density  $\psi$  depend on those of the surface  $\Gamma$  and the data  $v$ .

*Remarks 7.2.*

1. Aside from the restriction of solvability, the parameters  $\theta$  and  $\phi$  are arbitrary and can be exploited. For example,  $\theta \in (0, 1)$  and  $\phi \in [0, \phi_\Gamma]$  might be chosen by some means to optimize the conditioning of the linear operator in (7.9).
2. Just like the Power and Miranda formulation, the current boundary integral equation in (7.9) is singularity-free in the case when  $\phi > 0$ . The singularity in the single-layer potential is removed by virtue of the parallel surface. The singularity in the kernel of the double-layer potential can be removed in a simple, standard way by employing a well-known integral identity [11, 28, 30, 31] (see section 8).
3. Just like the Hebeker formulation, the current boundary integral formulation is natural for bodies of arbitrary shape. It seems particularly well suited for long, uniform, tubular bodies with complicated topology. In this case, the maximum offset distance  $\phi_\Gamma$  can be explicitly identified as the tube radius, and  $\Gamma$  and  $\gamma$  would be parallel tubular surfaces of different radii centered on the same axial curve. In general, however, an explicit characterization of  $\phi_\Gamma$  is not necessary, and the formulation is valid for any type of body.
4. All three formulations can be viewed as extensions to Stokes flow of ideas developed in classic potential theory. The idea of taking a linear combination of single- and double-layer potentials was considered in the work of Günter [13], and the idea of moving the single-layer potential to an inner surface, or limit thereof, was suggested in the work of Mikhlin [23]. (Mikhlin explicitly considered an inner point-source, which can be interpreted as the limit of a single-layer potential as the inner surface is squeezed to a point.) Other generalized formulations could also be considered. For example, the Power and Miranda formulation can be generalized by using a continuous distribution of stokeslet and rotlet singularities over an inner surface.

**7.3. Proof of Theorem 7.1.** Assume  $\theta \in (0, 1)$  and consider the homogeneous version of (7.7). Replacing  $\psi$  by  $\psi^h$  for notational convenience, we have

$$(7.11) \quad \theta V[\gamma, \psi^h \circ \varphi](x_0) + (1 - \theta) \overline{W}[\Gamma, \psi^h](x_0) + (1 - \theta) \alpha \psi^h(x_0) = 0 \quad \forall x_0 \in \Gamma.$$

According to the Fredholm theory [19, 23], if (7.11) possesses only the trivial solution  $\psi^h = 0$ , then (7.7) possesses a unique continuous solution  $\psi$  for any continuous data  $v$ . To show that  $\psi^h = 0$  is the only solution of (7.11), we proceed in four steps.

(1) Let  $\psi^h$  be an arbitrary solution of (7.11), and introduce fields  $(u^{(1)}, p^{(1)})$  and  $(u^{(2)}, p^{(2)})$  by

$$(7.12) \quad \begin{aligned} u^{(1)} &= (1 - \theta)W[\Gamma, \psi^h], & p^{(1)} &= (1 - \theta)P_W[\Gamma, \psi^h], \\ u^{(2)} &= -\theta V[\gamma, \psi^h \circ \varphi], & p^{(2)} &= -\theta P_V[\gamma, \psi^h \circ \varphi]. \end{aligned}$$

Then  $(u^{(1)}, p^{(1)})$  and  $(u^{(2)}, p^{(2)})$  satisfy the homogeneous Stokes equations (2.1)<sub>1,2,4</sub>



in  $B_e$ . Moreover, from (7.11) and the limit relation for  $W[\Gamma, \psi^h]$  in (4.5), we have

$$(7.13) \quad \lim_{\substack{x \rightarrow x_0 \\ x \in B_e}} u^{(1)}(x) - u^{(2)}(x) = 0 \quad \forall x_0 \in \Gamma.$$

Thus  $u^{(1)} = u^{(2)}$  on  $\Gamma$ , and by uniqueness of solutions of the boundary-value problem (2.1), we have  $(u^{(1)}, p^{(1)}) = (u^{(2)}, p^{(2)})$  in  $B_e$ . Furthermore, by properties of the single- and double-layer potentials defined in (4.1) and (4.2), we have  $u^{(1)} = O(|x|^{-2})$  and  $u^{(2)} = O(|x|^{-1})$  as  $|x| \rightarrow \infty$ , and  $p^{(1)} = O(|x|^{-3})$  and  $p^{(2)} = O(|x|^{-2})$ . Thus we deduce

$$(7.14) \quad u^{(1)} = u^{(2)} = 0 \quad \text{and} \quad p^{(1)} = p^{(2)} = 0 \quad \forall x \in B_e.$$

(2) Since  $u^{(1)} = 0$  in  $B_e$  and  $1 - \theta \neq 0$ , we deduce from (7.12) that  $W[\Gamma, \psi^h] = 0$  in  $B_e$ , which implies

$$(7.15) \quad \lim_{\substack{x \rightarrow x_0 \\ x \in B_e}} W[\Gamma, \psi^h](x) = 0 \quad \forall x_0 \in \Gamma.$$

Using the limit relation in (4.5), we get

$$(7.16) \quad \overline{W}[\Gamma, \psi^h](x_0) + \alpha \psi^h(x_0) = 0 \quad \forall x_0 \in \Gamma.$$

By well-known properties of the double-layer potential [20, 26], the above equation possesses exactly six independent eigenfunctions  $\psi^{h,(1)}, \dots, \psi^{h,(6)}$  defined for  $x \in \Gamma$  by

$$(7.17) \quad \begin{aligned} \psi_i^{h,(a)}(x) &= \delta_{ia}, & a &= 1, 2, 3, \\ \psi_i^{h,(a)}(x) &= \varepsilon_{ij(a-3)} x_j, & a &= 4, 5, 6. \end{aligned}$$

Thus every solution  $\psi^h$  of (7.11) satisfies (7.16) and must necessarily be of the form

$$(7.18) \quad \psi^h(x) = \sum_{a=1}^6 c_a \psi^{h,(a)}(x),$$

where  $c_1, \dots, c_6$  are arbitrary constants.

(3) Since  $u^{(2)} = 0$  and  $p^{(2)} = 0$  in  $B_e$  and  $\theta \neq 0$ , we deduce from (7.12) that  $V[\gamma, \psi^h \circ \varphi] = 0$  and  $P_V[\gamma, \psi^h \circ \varphi] = 0$  in  $B_e$ . Thus the resultant force and torque, about an arbitrary point  $q$ , exerted on  $\Gamma$  by the exterior single-layer flow ( $V[\gamma, \psi^h \circ \varphi]$ ,  $P_V[\gamma, \psi^h \circ \varphi]$ ) must vanish. By properties of the single-layer potentials outlined in section 4.4, and considering that  $\gamma \subset \Gamma_{\text{int}}$  when  $\phi > 0$  and  $\gamma = \Gamma$  when  $\phi = 0$ , we find in both cases that

$$(7.19) \quad \begin{aligned} F_V[\gamma, \psi^h \circ \varphi] &= -8\pi \int_{\gamma} \psi^h(\varphi(\xi)) dA_{\xi} = 0, \\ T_V[\gamma, \psi^h \circ \varphi] &= -8\pi \int_{\gamma} (\xi - q) \times \psi^h(\varphi(\xi)) dA_{\xi} = 0. \end{aligned}$$

Dividing by  $-8\pi$  and substituting for  $\psi^h$  using (7.18) and (7.17), we find that the above equations yield a linear system for  $c = (c_1, \dots, c_6)$  of the form

$$(7.20) \quad \begin{bmatrix} A & B \\ C & D \end{bmatrix} c = 0,$$

where  $A, B, C, D \in \mathbb{R}^{3 \times 3}$  are defined by

$$(7.21) \quad \begin{aligned} A_{ij} &= \int_{\gamma} \delta_{ij} dA_{\xi}, & B_{ik} &= \int_{\gamma} \varepsilon_{ijk} \varphi_j(\xi) dA_{\xi}, \\ C_{ij} &= \int_{\gamma} \varepsilon_{ipj} (\xi_p - q_p) dA_{\xi}, & D_{ik} &= \int_{\gamma} \varepsilon_{ipl} \varepsilon_{ljk} (\xi_p - q_p) \varphi_j(\xi) dA_{\xi}. \end{aligned}$$

(4) For convenience, let the torque reference point  $q$  be the centroid of  $\gamma$ , and assume without loss of generality that  $q = 0$ . Then  $C_{ij} = 0$  and (7.20) will possess only the trivial solution provided that the matrix  $D_{ik}$  is invertible. Notice that the matrix  $A_{ij}$  is always invertible since  $\gamma$  has positive measure. With  $q = 0$  we have

$$(7.22) \quad D_{ik} = \int_{\gamma} \varepsilon_{ipl} \varepsilon_{ljk} \xi_p \varphi_j(\xi) dA_{\xi}.$$

Substituting  $\varphi(\xi) = \xi + \phi n(\xi)$ , where  $n$  is the outward unit normal field on  $\gamma$  (see section 7.1), and using the standard permutation symbol identity  $\varepsilon_{ipl} \varepsilon_{ljk} = \delta_{ij} \delta_{pk} - \delta_{ik} \delta_{pj}$ , we obtain

$$(7.23) \quad D_{ik} = \int_{\gamma} \xi_i \xi_k - \delta_{ik} \xi_j \xi_j dA_{\xi} + \phi \int_{\gamma} \xi_k n_i dA_{\xi} - \phi \delta_{ik} \int_{\gamma} \xi_j n_j dA_{\xi}.$$

Applying the divergence theorem to the last two integrals in the above equation, we get, after straightforward simplification,

$$(7.24) \quad D_{ik} = -[G_{ik} + 2\phi \text{vol}(\gamma_{\text{int}}) \delta_{ik}].$$

Here  $\text{vol}(\gamma_{\text{int}}) > 0$  is the volume of the interior domain enclosed by  $\gamma$  and  $G_{ik} = \int_{\gamma} \delta_{ik} |\xi|^2 - \xi_i \xi_k dA_{\xi}$  is the symmetric, positive-definite, second moment tensor associated with  $\gamma$ . Since  $D_{ik}$  is invertible for any  $\phi \geq 0$ , we deduce that (7.20) admits only the trivial solution  $c = 0$ . Combining this with (7.18), we deduce that (7.11) admits only the trivial solution  $\psi^h = 0$ . This completes the proof of Theorem 7.1.

**8. Nyström approximation.** In this section we describe a numerical method for the formulation presented in section 7. We outline a singularity-free formulation of the boundary integral equation for the unknown density, discretize it using a straightforward Nyström method with an arbitrary quadrature rule, and introduce corresponding discretizations for various flow quantities of interest.

**8.1. Singularity-free formulation.** Given arbitrary parameters  $\theta \in (0, 1)$  and  $\phi \in (0, \phi_{\Gamma})$ , the integral equation (7.9) can be written in the convenient form

$$(8.1) \quad \begin{aligned} \theta \int_{\Gamma} G(x, y) \psi(y) dA_y + (1 - \theta) \int_{\Gamma} H(x, y) \psi(y) dA_y \\ + (1 - \theta) \alpha \psi(x) = v(x) \quad \forall x \in \Gamma, \end{aligned}$$

where  $G_{ij}(x, y) = J^{\phi}(y) U_{ij}^{\text{PF}}(x, \zeta(y))$  is the regularized, bounded, single-layer kernel and  $H_{ij}(x, y) = U_{ij}^{\text{STR}}(x, y) \nu_l(y)$  is the standard, weakly-singular, double-layer kernel. The singularity in  $H(x, y)$  can be avoided in a simple way by exploiting the double-layer identity [11, 28, 30, 31]

$$(8.2) \quad \int_{\Gamma} H_{ij}(x, y) dA_y = -\alpha \delta_{ij} \quad \forall x \in \Gamma.$$

In particular, substitution of (8.2) into (8.1) gives

$$(8.3) \quad \theta \int_{\Gamma} G(x, y)\psi(y) dA_y + (1 - \theta) \int_{\Gamma} H(x, y)[\psi(y) - \psi(x)] dA_y = v(x) \quad \forall x \in \Gamma.$$

Assuming  $\nu$  and  $\psi$  are Lipschitz continuous and  $\Gamma$  is a Lyapunov surface, it can be shown that the functions  $G(x, y)\psi(y)$  and  $H(x, y)[\psi(y) - \psi(x)]$  are uniformly bounded for all  $x$  and  $y$  on  $\Gamma$ . Thus (8.3) is singularity-free and can be discretized by Nyström methods.

*Remarks 8.1.*

1. Following standard practice [28, 30, 31], we define  $H(x, y)[\psi(y) - \psi(x)]$  to be zero when  $y = x$ . This modification does not alter the value of the integral and is necessary to obtain a well-defined Nyström discretization, which requires a value for this function for arbitrary  $x$  and  $y$ . The results in [31] show that Nyström methods defined using this practice are, in general, convergent. However, there is generally an upper bound on the order of convergence of these methods because of the above modification.
2. There is some freedom in the treatment of the first term in (8.3). When written as an integral over  $\Gamma$  as above, the kernel function  $G(x, y)$  contains the factor  $J^\phi(y)$ , which depends on the curvature of  $\Gamma$  (see section 7.1). By a change of variable, this term could also be written as an integral over the parallel surface  $\gamma$ . In this case, the curvature factor disappears, but an explicit parameterization of  $\gamma$  becomes necessary.

**8.2. Approximation of integral equation.** We suppose  $\Gamma$  can be decomposed into a union of nonoverlapping patches  $\Gamma_p$ ,  $p = 1, \dots, M_p$ , where each patch is the image of a smooth map  $y = \chi_p(s, t) : D_p \rightarrow \mathbb{R}^3$ , and each  $D_p$  is a domain in  $\mathbb{R}^2$ . By subdividing each domain  $D_p$  into nonoverlapping subdomains  $D_p^e$ ,  $e = 1, \dots, M_e$ , we decompose each patch  $\Gamma_p$  into curved, nonoverlapping patch elements  $\Gamma_p^e$ . In each patch element we introduce quadrature points  $y_{p,e,q}$  and weights  $W_{p,e,q}$ ,  $q = 1, \dots, M_q$ , such that

$$(8.4) \quad \int_{\Gamma_p^e} f(y) dA_y = \int_{D_p^e} f(\chi_p(s, t))J_p(s, t) ds dt \approx \sum_{q=1}^{M_q} f(y_{p,e,q})W_{p,e,q}.$$

Here  $J_p$  is the Jacobian associated with the patch parameterization  $\chi_p$ , which is assumed to be included in the weights  $W_{p,e,q}$ .

Let  $\psi_{p,e,q}$  be an approximation to  $\psi(y_{p,e,q})$ , and for convenience let  $a$  and  $b$  denote values of the multi-index  $(p, e, q)$ . Then a Nyström discretization of (8.3) is

$$(8.5) \quad \theta \sum_b G_{ab}\psi_b W_b + (1 - \theta) \sum_{b \neq a} H_{ab}[\psi_b - \psi_a]W_b = v_a \quad \forall a,$$

where  $G_{ab} = G(x_a, y_b)$ ,  $H_{ab} = H(x_a, y_b)$ , and  $v_a = v(x_a)$ . Here the product  $H_{ab}[\psi_b - \psi_a]$  has been set equal to zero when  $b = a$ . The above equation can be written in the standard form

$$(8.6) \quad \sum_b A_{ab}\psi_b = v_a \quad \forall a,$$

where  $A_{ab} \in \mathbb{R}^{3 \times 3}$  are defined by

$$(8.7) \quad A_{ab} = \begin{cases} \theta G_{ab} W_b + (1 - \theta) H_{ab} W_b, & a \neq b, \\ \theta G_{aa} W_a - (1 - \theta) \sum_{c \neq a} H_{ac} W_c, & a = b. \end{cases}$$

Equation (8.6) is a linear system of algebraic equations for the approximate density values  $\psi_b$  at the quadrature points  $y_b$ . This system is dense and nonsymmetric and can be solved using any suitable numerical technique.

**8.3. Approximation of flow quantities.** Various flow quantities of interest take the form of an integral of  $\psi$  over  $\Gamma$ . For example, from (7.5), the resultant force and torque on  $\Gamma$  about an arbitrary point  $c$  are given by

$$(8.8) \quad F = -8\pi\theta \int_{\gamma} \psi(\varphi(\xi)) dA_{\xi}, \quad T = -8\pi\theta \int_{\gamma} (\xi - c) \times \psi(\varphi(\xi)) dA_{\xi}.$$

After a change of variable (see section 7.1), these integrals can be transformed from the parallel surface  $\gamma$  to the body surface  $\Gamma$  to obtain

$$(8.9) \quad F = -8\pi\theta \int_{\Gamma} J^{\phi}(y) \psi(y) dA_y, \quad T = -8\pi\theta \int_{\Gamma} J^{\phi}(y) (\zeta(y) - c) \times \psi(y) dA_y.$$

By discretizing these integrals using the same quadrature points and weights as before, we get the approximations

$$(8.10) \quad F^{\text{approx}} = -8\pi\theta \sum_b J_b^{\phi} \psi_b W_b, \quad T^{\text{approx}} = -8\pi\theta \sum_b J_b^{\phi} (\zeta_b - c) \times \psi_b W_b.$$

An approximation to the volume flow rate  $Q$  associated with  $\Gamma$  can be obtained in a similar manner.

**9. Numerical experiments.** Here we present results from numerical experiments on three different bodies: a sphere, torus, and helical tube with hemispherical endcaps. For one or more prescribed motions of each body, we computed the resultant force and torque about the origin of a body-fixed frame and examined various measures of convergence.

**9.1. Methods.** Following the general procedure outlined above, we decomposed the surface of each body into nonoverlapping patches  $\Gamma_p$ , each parameterized over a rectangular domain  $D_p$ . We subdivided each patch into curved, quadrilateral elements  $\Gamma_p^e$ , and in each element we used an  $m \times m$  tensor product Gauss–Legendre quadrature rule, with order of accuracy  $r_{\text{abs}} = 2m$  on absolute errors. For the sphere we employed six patches based on stereographic projection from the faces of a bounding cube. For the torus we employed a single patch based on an explicit parameterization of the axial curve. For the helical tube we employed multiple patches based on explicit parameterizations of the axial curve and endcaps.

The resultant force  $F$  and torque  $T$  on each body were computed by solving the linear algebraic system (8.6) of size  $(3M_p M_e M_q) \times (3M_p M_e M_q)$ . Because this system is nonsymmetric and was observed to be well conditioned, we used the GMRES iterative solver implemented in MATLAB with no preconditioning and a residual tolerance of  $10^{-12}$ . Using the solution of (8.6), we computed approximations to  $F$  and  $T$  according to (8.10). The total number of quadrature points,  $M_p M_e M_q$ , was varied up to a maximum value of 4000 to 8000 depending on the example. All computations were performed with the parameter values  $\theta = 1/2$  and  $\phi/\phi_{\Gamma} = 1/2$ , where  $\phi_{\Gamma}$  is the maximum offset distance for the parallel surface associated with  $\Gamma$ .

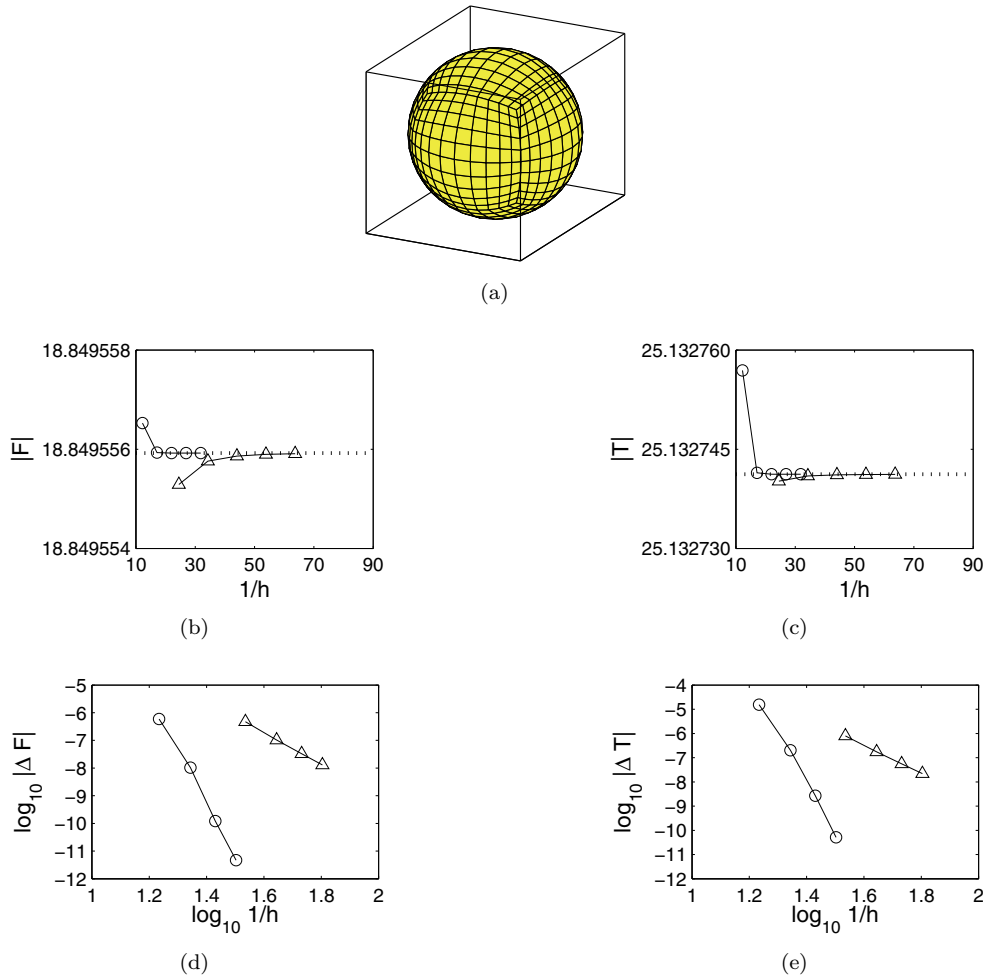


FIG. 9.1. Convergence results for resultant force  $F$  and torque  $T$  on a sphere. Computations were performed with a sequence of meshes with element sizes  $h_k$ . (a) Sample mesh. (b),(c) Plots of  $|F_{h_k}|$  and  $|T_{h_k}|$  versus  $1/h_k$  for the translational and rotational motion, respectively. The dotted horizontal lines indicate exact values. (d),(e) Plots of  $\log_{10} |F_{h_k} - F_{h_{k-1}}|$  and  $\log_{10} |T_{h_k} - T_{h_{k-1}}|$  versus  $\log_{10}(1/h_k)$  for the translational and rotational motion, respectively. In all plots, triangles denote results for the  $1 \times 1$  quadrature rule, and circles denote results for the  $2 \times 2$  rule.

**9.2. Results.** Figure 9.1 shows convergence results for the resultant force and torque about the origin on a sphere obtained with the  $1 \times 1$  and  $2 \times 2$  quadrature rules. The sphere had a radius  $r = 1$  and was centered at the origin. For this surface, the maximum signed curvature is  $\kappa_\Gamma = 1/r$ , which gives a maximum offset distance of  $\phi_\Gamma = r$ . Results are given for two independent boundary conditions—translation along the  $x$ -axis with unit velocity, and rotation about the same axis with unit angular velocity. In these cases, exact values are known:  $F = (-6\pi, 0, 0)$  and  $T = (0, 0, 0)$  for the translational motion, and  $F = (0, 0, 0)$  and  $T = (-8\pi, 0, 0)$  for the rotational motion.

Plot (a) of Figure 9.1 illustrates the geometry and a sample mesh. In our computations, a sequence of five increasingly refined meshes were considered for each

quadrature rule, with each mesh being relatively uniform. The meshes were chosen such that, at each stage in the sequence, the linear algebraic systems for the  $1 \times 1$  and  $2 \times 2$  quadrature rules were approximately the same size. The mesh shown in (a) is the coarsest used with the  $1 \times 1$  rule. Plot (b) shows convergence results for the magnitude of  $F$  in the translational motion as a function of the element size parameter  $h$ , defined by  $M_p M_e h^2 = 1$ , where  $M_p M_e$  is the total number of elements in a mesh. In particular,  $h$  is proportional to the average element size. Plot (c) shows similar convergence results for the magnitude of  $T$  in the rotational motion. In all computations, the appropriate entries in both  $F$  and  $T$  were found to be zero within machine precision for each type of motion. Thus the errors illustrated can be attributed to the appropriate nonzero components.

Plot (d) of Figure 9.1 shows the difference in the computed values of  $F$  between successive meshes as a function of  $h$  for the translational motion. Although an exact solution is available, we consider solution differences rather than absolute errors for purposes of later comparison. Plot (e) shows similar results for the difference in the computed values of  $T$  for the rotational motion. For an  $m \times m$  Gauss–Legendre quadrature rule, the convergence rate  $r_{\text{diff}}$  for solution differences is expected to be  $2m + 1$ , which is one order higher than the standard convergence rate  $r_{\text{abs}}$  for absolute errors. The plots show that the observed convergence rate for solution differences was significantly higher than expected. Considering both  $F$  and  $T$ , we have  $5 \leq r_{\text{diff}} \leq 6$  for  $m = 1$  and  $19 \leq r_{\text{diff}} \leq 20$  for  $m = 2$ . On the finest two meshes used with the  $2 \times 2$  rule, the relative change in  $F$  for the translational motion was of order  $10^{-13}$ , and the relative change in  $T$  for the rotational motion was of order  $10^{-12}$ .

Figure 9.2 shows convergence results for the resultant force and torque about the origin on a torus. The axial curve of the torus was a circle of radius  $\rho = 1$  centered at the origin in the  $xy$ -plane, and the tube section was a circle of radius  $r = \rho(1 - \eta)/(1 + \eta)$ , where  $\eta = \tanh^2(1)$ . This value of the tube radius was chosen to compare results against an exact solution from [34]. For this surface, the maximum signed curvature is  $\kappa_\Gamma = 1/r$ , which gives a maximum offset distance of  $\phi_\Gamma = r$ . Results are given for two independent boundary conditions—translation along the  $z$ -axis with unit velocity, and rotation about the same axis with unit angular velocity. Symmetry implies that the force and torque have the form  $F = (0, 0, F_z)$  and  $T = (0, 0, 0)$  for the translational motion and  $F = (0, 0, 0)$  and  $T = (0, 0, T_z)$  for the rotational motion. For the translational motion, the force  $F_z$  has been characterized, and its approximate numerical value is  $F_z = -20.7379$  [34]. For the rotational motion, the torque  $T_z$  has also been characterized [16], but its approximate numerical value does not appear to be well known.

Plots (a) through (e) of Figure 9.2 are analogous to the previous example. In our computations, we again found that the appropriate entries in both  $F$  and  $T$  were zero within machine precision for each type of motion. Moreover, the observed convergence rate for solution differences was again higher than expected. Considering both  $F$  and  $T$ , we have  $9 \leq r_{\text{diff}} \leq 16$  for  $m = 1$  and  $6 \leq r_{\text{diff}} \leq 8$  for  $m = 2$ . Interestingly, for the range of meshes considered here, the  $1 \times 1$  rule performed better than the  $2 \times 2$  rule. On the finest two meshes used with the  $1 \times 1$  rule, the relative change in  $F$  for the translational motion was of order  $10^{-9}$ , and the relative change in  $T$  for the rotational motion was of order  $10^{-6}$ .

Figure 9.3 shows convergence results for the resultant force and torque about the origin on a helical tube. The axial curve of the tube was a helical curve about the  $z$ -axis with radius  $\rho = 2$ , pitch  $\lambda = 3$ , and arclength  $l = 2\pi$ . The tube had uniform, circular cross-sections of radius  $r = 0.2$  and hemispherical endcaps of the

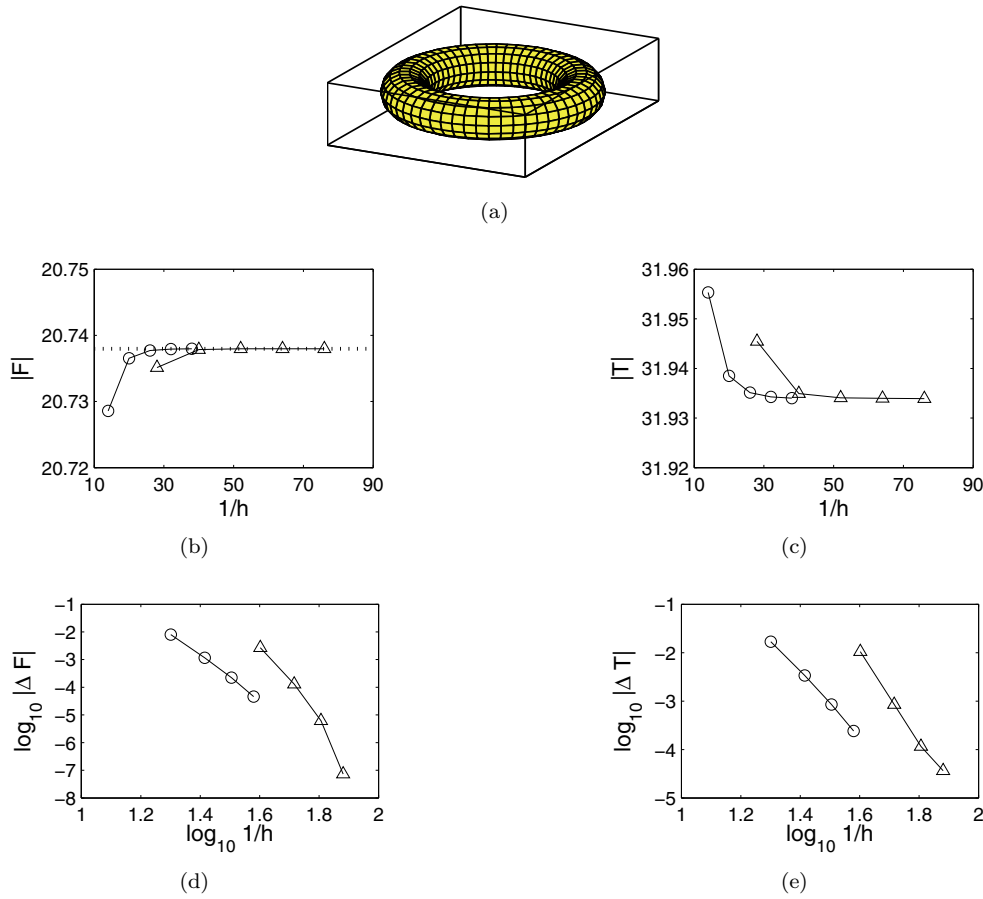


FIG. 9.2. Convergence results for resultant force  $F$  and torque  $T$  on a torus. Computations were performed with a sequence of meshes with element sizes  $h_k$ . (a) Sample mesh. (b),(c) Plots of  $|F_{h_k}|$  and  $|T_{h_k}|$  versus  $1/h_k$  for the translational and rotational motion, respectively. The dotted horizontal line in (b) indicates an exact value. (d),(e) Plots of  $\log_{10} |F_{h_k} - F_{h_{k-1}}|$  and  $\log_{10} |T_{h_k} - T_{h_{k-1}}|$  versus  $\log_{10}(1/h_k)$  for the translational and rotational motion, respectively. In all plots, triangles denote results for the  $1 \times 1$  quadrature rule, and circles denote results for the  $2 \times 2$  rule.

same radius. These geometrical parameters were chosen so as to produce a tubular body of moderately high curvature. As with the torus, the maximum signed curvature is  $\kappa_\Gamma = 1/r$ , which gives a maximum offset distance of  $\phi_\Gamma = r$ . In contrast to the previous two examples, results are given for a single boundary condition—rotation about the  $x$ -axis with unit angular velocity. In this case, the resultant force and torque are not known exactly and are not known to have any special form.

Plots (a) through (e) of Figure 9.3 are analogous to the previous two examples, with the exception that only one type of motion is considered. For this single motion the force and torque were each found to possess three nonzero components, in contrast to the previous examples. The observed convergence rate for solution differences was again higher than expected. Considering both  $F$  and  $T$ , we have  $3 \leq r_{\text{diff}} \leq 6$  for  $m = 1$  and  $8 \leq r_{\text{diff}} \leq 10$  for  $m = 2$ . For  $T$  we notice that the results from the  $2 \times 2$  rule converge to a limiting value monotonically from below, whereas the results from the  $1 \times 1$  rule converge nonmonotonically from above. On the finest two meshes used

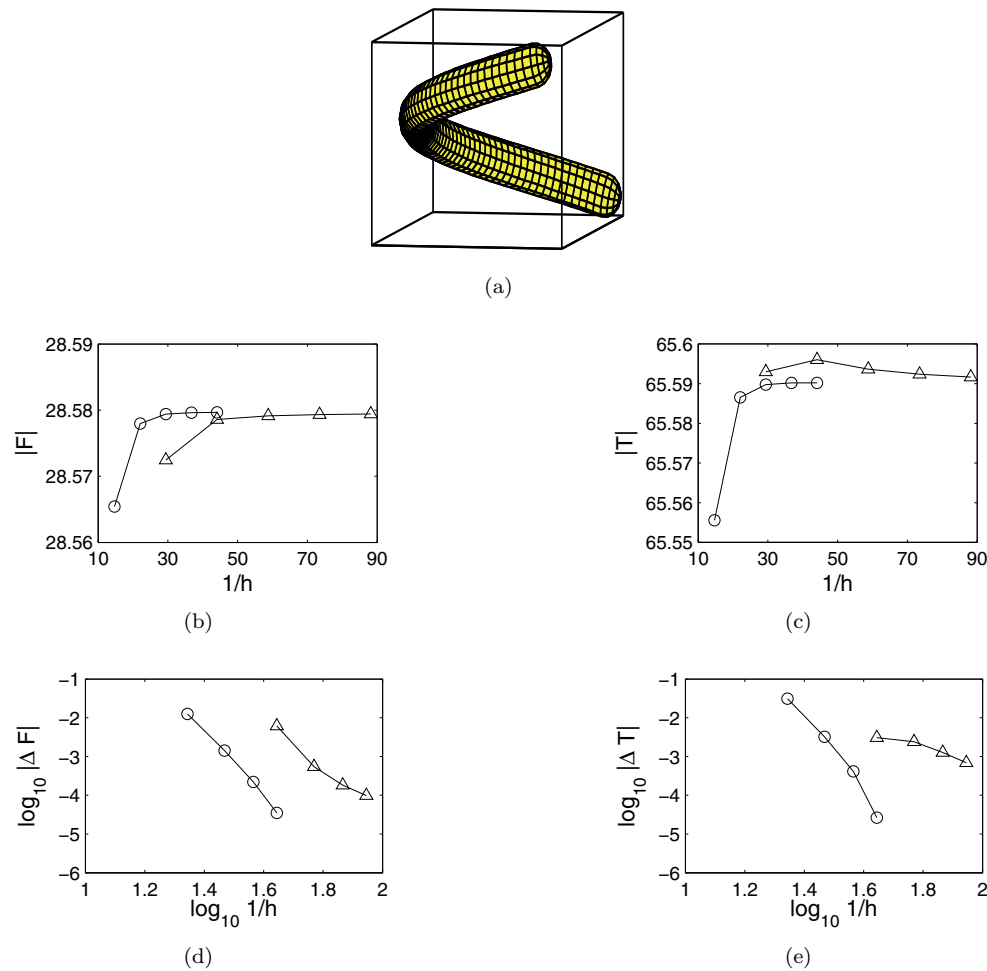


FIG. 9.3. Convergence results for resultant force  $F$  and torque  $T$  on a helical tube. Computations were performed with a sequence of meshes with element sizes  $h_k$ . (a) Sample mesh. (b),(c) Plots of  $|F_{h_k}|$  and  $|T_{h_k}|$  versus  $1/h_k$ . (d),(e) Plots of  $\log_{10} |F_{h_k} - F_{h_{k-1}}|$  and  $\log_{10} |T_{h_k} - T_{h_{k-1}}|$  versus  $\log_{10}(1/h_k)$ . In all plots, triangles denote results for the  $1 \times 1$  quadrature rule, and circles denote results for the  $2 \times 2$  rule.

with the  $2 \times 2$  rule, the relative change in  $F$  was of order  $10^{-6}$ , and the relative change in  $T$  was of order  $10^{-7}$ .

**9.3. Discussion.** The examples outlined above suggest that the singularity-free boundary integral formulation introduced here leads to a viable numerical scheme for exterior Stokes flow problems. Issues associated with weakly singular integrals are avoided in a simple and efficient way without the need for product integration rules or specialized coordinate transformations and projections. In all three examples, the schemes exhibited convergence rates that were higher than expected and produced reasonably accurate results with reasonable meshes. For meshes of comparable size, the results for the torus and helical tube examples were less accurate than those for the sphere example. This is likely due to the relatively high curvature and more complicated shapes of the torus and helical tube. As can be expected, finer meshes



are needed in these cases to achieve a level of accuracy similar to that for the sphere. The role of the parameters  $\theta$  and  $\phi$  in the conditioning and performance of these schemes for different classes of bodies will be investigated in a separate work.

**Acknowledgments.** The author thanks the reviewers for their helpful comments and the National Science Foundation for its generous support.

## REFERENCES

- [1] B. ALPERT, G. BEYLKIN, R. COIFMAN, AND V. ROKHLIN, *Wavelet-like bases for the fast solution of second-kind integral equations*, SIAM J. Sci. Comput., 14 (1993), pp. 159–184.
- [2] K. E. ATKINSON, *The numerical solution of Laplace's equation in three dimensions*, SIAM J. Numer. Anal., 19 (1982), pp. 263–274.
- [3] K. E. ATKINSON, *The Numerical Solution of Integral Equations of the Second Kind*, Cambridge University Press, Cambridge, UK, 1997.
- [4] G. K. BATCHELOR, *Slender-body theory for particles of arbitrary cross-section in Stokes flow*, J. Fluid Mech., 44 (1970), pp. 419–440.
- [5] C. BREBBIA, J. TELLES, AND L. WROBEL, *Boundary Element Techniques*, Springer-Verlag, New York, 1984.
- [6] G. CHEN AND J. ZHOU, *Boundary Element Methods*, Academic Press, New York, 1992.
- [7] T. A. DABROS, *Singularity method for calculating hydrodynamic forces and particle velocities in low-Reynolds-number flows*, J. Fluid Mech., 156 (1985), pp. 1–21.
- [8] M. G. DUFFY, *Quadrature over a pyramid or cube of integrands with a singularity at a vertex*, SIAM J. Numer. Anal., 19 (1982), pp. 1260–1262.
- [9] R. FINN, *On the exterior stationary problem for the Navier-Stokes equations and associated perturbation problems*, Arch. Ration. Mech. Anal., 19 (1965), pp. 363–406.
- [10] M. GANESH, I. G. GRAHAM, AND J. SIVALOGANATHAN, *A new spectral boundary integral collocation method for three-dimensional potential problems*, SIAM J. Numer. Anal., 35 (1998), pp. 778–805.
- [11] M. A. GOLDBERG AND C. S. CHEN, *Discrete Projection Methods for Integral Equations*, Computational Mechanics Publications, Billerica, MA, 1997.
- [12] I. G. GRAHAM AND I. H. SLOAN, *Fully discrete spectral boundary integral methods for Helmholtz problems on smooth closed surfaces in  $\mathbb{R}^3$* , Numer. Math., 92 (2002), pp. 289–323.
- [13] N. M. GÜNTER, *Potential Theory and Its Applications to Basic Problems of Mathematical Physics*, Frederick Ungar Publishing, New York, 1967.
- [14] F. K. HEBEKER, *A boundary element method for Stokes equations in 3-D exterior domains*, in The Mathematics of Finite Elements and Applications V, J. R. Whiteman, ed., Academic Press, London, 1985, pp. 257–263.
- [15] R. E. JOHNSON, *An improved slender-body theory for Stokes flow*, J. Fluid Mech., 99 (1980), pp. 411–431.
- [16] R. P. KANWAL, *Slow steady rotation of axially symmetric bodies in a viscous fluid*, J. Fluid Mech., 10 (1961), pp. 17–24.
- [17] J. B. KELLER AND S. I. RUBINOW, *Slender-body theory for slow viscous flow*, J. Fluid Mech., 75 (1976), pp. 705–714.
- [18] S. KIM AND S. J. KARRILA, *Microhydrodynamics*, Butterworth-Heinemann Publishing, Oxford, UK, 1991.
- [19] R. KRESS, *Linear Integral Equations*, Appl. Math. Sci. 82, Springer-Verlag, New York, 1989.
- [20] O. A. LADYZHENSKAYA, *The Mathematical Theory of Viscous Incompressible Flow*, revised English ed., Gordon and Breach, New York, 1963.
- [21] C. LAGE AND C. SCHWAB, *Wavelet Galerkin algorithms for boundary integral equations*, SIAM J. Sci. Comput., 20 (1999), pp. 2195–2222.
- [22] P. A. MARTIN, *Multiple Scattering*, Encyclopedia Math. Appl. 107, Cambridge University Press, Cambridge, UK, 2006.
- [23] S. G. MIKHLIN, *Linear Integral Equations*, International Monographs on Advanced Mathematics and Physics, Hindustan Publishing Corporation, Delhi, 1960.
- [24] S. G. MIKHLIN, *Multidimensional Singular Integrals and Integral Equations*, International Series of Monographs in Pure and Applied Mathematics 83, Pergamon Press, Oxford, UK, 1965.
- [25] S. G. MIKHLIN AND S. PRÖSSDORF, *Singular Integral Operators*, Springer-Verlag, New York, 1986.

- [26] F. K. G. ODQVIST, *Über die randwertaufgaben der hydrodynamik zäher flüssigkeiten*, Math. Z., 32 (1930), pp. 329–375.
- [27] B. O'NEILL, *Elementary Differential Geometry*, Academic Press, New York, 1966.
- [28] H. POWER AND G. MIRANDA, *Second kind integral equation formulation of Stokes' flows past a particle of arbitrary shape*, SIAM J. Appl. Math., 47 (1987), pp. 689–698.
- [29] H. POWER AND L. C. WROBEL, *Boundary Integral Methods in Fluid Mechanics*, Computational Mechanics Publications, Billerica, MA, 1995.
- [30] C. POZRIKIDIS, *Boundary Integral and Singularity Methods for Linearized Viscous Flow*, Cambridge University Press, Cambridge, UK, 1992.
- [31] A. RATHSFELD, *Quadrature methods for 2D and 3D problems*, J. Comput. Appl. Math., 125 (2000), pp. 439–460.
- [32] J. TAUSCH AND J. WHITE, *Multiscale bases for the sparse representation of boundary integral operators on complex geometry*, SIAM J. Sci. Comput., 24 (2003), pp. 1610–1629.
- [33] L. YING, G. BIROS, AND D. ZORIN, *A high-order 3D boundary integral equation solver for elliptic PDEs in smooth domains*, J. Comput. Phys., 219 (2006), pp. 247–275.
- [34] M. ZABARANKIN AND P. KROKHMAL, *Generalized analytic functions in 3D Stokes flows*, Quart. J. Mech. Appl. Math., 60 (2007), pp. 99–123.